Chapter 3

Tail effects in the 3PN gravitational wave energy flux of inspiralling compact binaries

3.1 Introduction

The GW energy flux from a system of two point masses in elliptic motion in the leading quadrupolar approximation (Newtonian order) was first discussed by Peters and Mathews [138, 112]. Using the Damour-Deruelle [147] 1PN quasi-Keplerian representation, Blanchet and Schafer [143] computed the 1PN corrections to the above result. Using the generalized quasi-Keplerian representation of Damour, Schafer and Wex [148, 149, 150], Gopakumar and Iyer extended these results to 2PN order [46]. Recently, Damour, Gopakumar and Iyer [47] proposed an analytic method based on an improved "method of variation of constants" to construct high accuracy templates for the GW signals from the inspiral phase of compact binaries moving in quasi-elliptical orbits. The three time scales related to orbital motion, precession and radiation reaction are handled without the usual approximation of assuming adiabaticity relative to the radiation reaction time scale. The above results relate to 2.5PN GW phasing. More recently they have been extended by Koenigsdoerffer and Gopakumar [163] to 3.5PN order. All these works above relate only to the *instantaneous* terms in the gravitational waves (GW).

The multipole moments describing gravitational waves emitted by an isolated system cannot evolve independently. They couple to each other and with themselves, giving rise to non-linear physical effects. Consequently, the above instantaneous terms in the flux must be supplemented by the contributions arising from these non-linear multipole interactions. The leading multipole interaction is between the mass quadrupole moment M_{ij} and the mass

monopole M or ADM mass. It is associated with the non-linear effect of tails at order 1.5PN. Physically it is due to the backscatter of linear waves from the space-time curvature generated by the mass monopole M. Tails imply a non-locality in time since they are described as integrals depending on the history of the source from the remote past to the current retarded time. They are thus appropriately referred to as hereditary contributions by Blanchet and Damour [63, 76]: terms nonlocal in time depending on the dynamics of the system in its entire past [76]. The most detailed study of tails is due to Blanchet [158, 157] based on the multipolar post-Minkowskian formalism of Blanchet and Damour [62, 64]. He showed that up to 3PN these comprise the dominant quadratic order tails, the cubic-order tails or tails of tails and the non-linear memory integral [164, 165, 166, 110]. The cubic "monopole-monopole-quadrupole" interaction represents the scattering of the linear quadrupole waves from the second-order (M^2) potential barrier of the Schwarzschild metric, and also the scattering of the quadratic tails off the first-order (M) potential barrier. The latter effect is called "tails of tails" of gravitational waves. See [158, 157] for earlier references to the general topic of tails and in particular to tails in the test-mass limit. In this chapter we set up a general theoretical framework to compute the hereditary contributions for binaries moving in elliptical orbits and apply it to evaluate all the tail contributions contained in the 3PN accurate GW energy flux.

For the instantaneous terms in the energy flux, explicit closed form analytical expressions can be given in terms of dynamical variables related to relative speed v and relative separation r. Consequently, these expressions can be conveniently averaged in the time domain over an orbit using its quasi-Keplerian representation. For the hereditary contribution on the other hand one can only write down formal analytical expressions as integrals over the past. More explicit expressions in terms of the dynamical variables require in addition a model of the binary's orbit to implement the integration over the past history. In the circular orbit case, with a simplified model of binary inspiral one can work directly in the time domain. For instance, Blanchet computed the hereditary terms in the flux upto 3.5PN [158, 157] while Arun, Blanchet, Iyer and Qusailah [110] evaluated the GW polarisations upto 2.5PN. The tail integrals are evaluated using standard integrals for a *fixed* non-decaying circular orbit. 'Remote-past' contribution to the tail integrals can be proved to be negligible and errors due to inspiral by gravitation radiation reaction to be at least 4PN. In the elliptic orbit case on the other hand the situation is more involved. Even after using the quasi-Keplerian parametrization, one cannot perform the integrals in the time domain (as for the circular orbit case), since the multipole moments have a more complicated dependence on time so that the integrals are not analytically solvable in simple closed forms. By working in the Fourier domain to explicitly evaluate the hereditary integrals, Blanchet and Schafer [145] computed the hereditary tail terms at 1.5PN for elliptical orbits using the lowest order Newtonian Kep-

lerian representation.

In the present investigation to tackle the terms at 2.5PN and 3PN we need to go beyond the (Newtonian) Keplerian representation to a 1PN quasi-Keplerian representation of the orbit. Here we encounter two further complications. Firstly, the 1PN parametrization of the binary involves three kinds of eccentricities (e,, e_t and e_ϕ) which makes the algebra more involved. More seriously at 1PN order, the periastron precession effect appears in the problem and one has to contend with two times scales: the orbital time scale and the periastron precession time scale. These two new features should be properly accounted for in the calculations to extend the Fourier methods in [145]. This strategy has been proposed and used earlier in computing the instantantaneous terms in the GW polarizations from binaries on elliptical orbits [83, 115, 47]. We shall adapt these features here to treat the more involved hereditary contribution to the total energy flux.

Following [145], we express all the multipole moments needed for the hereditary computation at Newtonian order as discrete Fourier series in l. However, for moments needed beyond the lowest Newtonian order the double periodicity needs to be crucially incorporated. The evaluation of the Fourier coefficients is done either numerically or in terms of an infinite sum of combinations of Bessel functions. All tail terms at 2.5PN and 3PN are completely computed to provide the 'enhancement factors' for binaries in elliptical orbits at the 2.5PN and 3PN orders, extending the classic work of Peters and Mathews [138]. The present work extends the circular orbit results at 2.5PN [156] and 3PN [95] to the elliptical orbit case. It also extends results for hereditary contributions at 1.5PN [145] for elliptical orbits to 2.5PN order and 3PN. The 3PN hereditary contributions comprise the tail-of-tails and tail-squared terms and are extensions of [157, 158] for circular orbits to the elliptical case. Combining the hereditary contributions computed in this chapter with the instantaneous contributions computed in the previous chapter yields the complete 3PN energy flux. The final expressions represent gravitational waves from a binary evolving negligibly under gravitational radiation reaction, including precisely upto 3PN order the effects of eccentricity and periastron precession during epochs of inspiral when the orbital parameters are essentially constant over a few orbital revolutions. It thus represents the first input to go towards the quasi-elliptical case; the evolution of the binary in a elliptical orbit under gravitational radiation reaction. Tails are not just mathematical curiosities in general relativity but facets that should show up in the gravitational-wave signals of inspiraling compact binaries and subsequently decoded by the GW detectors like VIRGO, LIGO and LISA [167, 168, 169, 170].

3.2 Tail terms in the 3PN energy flux

Three kinds of hereditary terms appear in the computation presented here. The 'tails' coming from the multipole interaction of the mass quadrupole with the ADM mass (M x I_{ij}), the 'tails of tails' due to the cubic nonlinear interaction M × M x I_{ij} and the tail-squared term arising from quadrupole-quadrupole interaction $I_{ij} \times I_{kl}$. In the equations to follow, we list the expressions for the hereditary terms constituting the fluxes. The hereditary terms in the energy flux can be written as

$$\left(\frac{d\mathcal{E}}{dt}\right)_{\text{hered}} = \left(\frac{d\mathcal{E}}{dt}\right)_{\text{tail}} + \left(\frac{d\mathcal{E}}{dt}\right)_{\text{tail(tail)}} + \left(\frac{d\mathcal{E}}{dt}\right)_{(\text{tail})^2} \tag{3.1}$$

where

$$\begin{aligned}
\left(\frac{d\mathcal{E}}{dt}\right)_{\text{tail}} = {} & \frac{4G^2M}{c^5}\left\{\frac{1}{5c^3}M_{ij}^{(3)}\int_0^{+\infty}d\tau M_{ij}^{(5)}(T_R-\tau)\left[\ln\left(\frac{c\tau}{2r_0}\right)+\frac{11}{12}\right]\right. \\
& +\frac{1}{189c^5}M_{ijk}^{(4)}\int_0^{+\infty}d\tau M_{ijk}^{(6)}(T_R-\tau)\left[\ln\left(\frac{c\tau}{2r_0}\right)+\frac{97}{60}\right] \\
& +\frac{16}{45c^5}S_{ij}^{(3)}\int_0^{+\infty}d\tau\, S_{ij}^{(5)}(T_R-\tau)\left[\ln\left(\frac{c\tau}{2r_0}\right)+\frac{7}{6}\right] \\
& +\frac{1}{9072c^7}M_{ijkl}^{(5)}\int_0^{+\infty}d\tau\, M_{ijkl}^{(7)}(T_R-\tau)\left[\ln\left(\frac{c\tau}{2r_0}\right)+\frac{59}{30}\right] \\
& +\frac{1}{84c^7}S_{ijk}^{(4)}\int_0^{+\infty}d\tau\, S_{ijk}^{(6)}(T_R-\tau)\left[\ln\left(\frac{c\tau}{2r_0}\right)+\frac{5}{3}\right] \\
& \left.+O\left(\frac{1}{c^8}\right)\right\}, \qquad (3.2a)
\end{aligned}$$

$$\begin{aligned}
\left(\frac{d\mathcal{E}}{dt}\right)_{\text{tail(tail)}} = {} & \frac{4G^2M}{c^5}\left\{\frac{GM}{5c^6}M_{ij}^{(3)}\int_0^{+\infty}d\tau M_{ij}^{(6)}(T_R-\tau)\right. \\
& \left.\times\left[\ln^2\left(\frac{c\tau}{2r_0}\right)+\frac{57}{70}\ln\left(\frac{c\tau}{2r_0}\right)+\frac{124627}{44100}\right]+O\left(\frac{1}{c^8}\right)\right\}, \qquad (3.2b)
\end{aligned}$$

$$\begin{aligned}
\left(\frac{d\mathcal{E}}{dt}\right)_{(\text{tail})^2} = {} & \frac{4G^2M}{c^5}\left\{\frac{GM}{5c^6}\left(\int_0^{+\infty}d\tau M_{ij}^{(5)}(T_R-\tau)\left[\ln\left(\frac{c\tau}{2r_0}\right)+\frac{11}{12}\right]\right)^2\right. \\
& \left.+O\left(\frac{1}{c^{10}}\right)\right\}. \qquad (3.2c)
\end{aligned}$$

The constant scaling the logarithm has been chosen to be r_0 to match with the choice made in the computation of tails-of-tails in [158]. It is a freely specifiable constant, entering the relation between the retarded time $U = \mathrm{T} - R/c$ in radiative coordinates and the corresponding time $t - \rho/c$ in harmonic coordinates (where ρ is the distance of the source in harmonic

coordinates). More precisely we have

$$U = t - \frac{\rho}{c} - \frac{2GM}{c^3}\ln\left(\frac{\rho}{c\,r_0}\right). \tag{3.3}$$

In this chapter, in what follows, we set $c = 1$ and G = 1.

3.3 Solution of the equations of motion of compact binaries

In this chapter as in the the previous one, we shall often need to use the explicit solution for the motion of compact binary systems in the post-Newtonian approximation. We review here the relevant material we need, which includes the general doubly-periodic structure of the post-Newtonian solution, and the quasi-Keplerian representation of the 1PN binary motion by means of different types of eccentricities. We closely follow the works of Damour [65, 83] and Damour & Deruelle [147, 171].

3.3.1 Doubly-periodic structure of the solution

The equations of motion of a compact binary system up to the 3PN order admit, when neglecting the radiation reaction term at the 2.5PN order, ten first integrals of the motion corresponding to the conservation of energy, angular and linear momenta, and center-of-mass position [160]. When restricted to the frame of the center of mass, the equations admit four first integrals associated with the energy E and angular momentum J, given at 3PN order by Eqs. (4.8)–(4.9) of Ref. [159].

The motion takes place in the plane orthogonal to J. Denoting by r the binary's orbital separation in that plane, and by $v = \mathbf{v}_1 - \mathbf{v}_2$ the relative velocity, we find that E together with the norm $J = |\mathbf{J}|$ are functions of r, $\dot{r}^2$ and v^2 (we are employing the harmonic coordinate system of [159]). They depend also on the total mass $m = m_1 + m_2$ and reduced mass $\mu = m_1 m_2/m$. We adopt polar coordinates r, ϕ in the orbital plane, and express E and J, thanks to $v^2 = \dot{r}^2 + r^2\dot{\phi}^2$, as some explicit functions of r, $\dot{r}^2$ and $\dot{\phi}$. The latter functions can be inverted (by means of straightforward post-Newtonian iteration) to give $\dot{r}^2$ and $\dot{\phi}$ in terms of r and the constants of motion E and J. Hence,

$$\dot{r}^2 = \mathcal{R}[r; \mathrm{E}, \mathrm{J}], \tag{3.4a}$$

$$\dot{\phi} = \mathcal{G}[r; E, \mathrm{Jl}, \tag{3.4b}$$

where the functions $\mathcal{R}$ and $\mathcal{G}$ denote certain polynomials in $1/r$, the degree of which depends on the post-Newtonian approximation in question (it is seventh degree for both $\mathcal{R}$ and $\mathcal{G}$ at

3PN order [155]). The various coefficients of the powers of $1/r$ are themselves polynomials in E and J, and also of course depend on m and the mass ratio $\nu = \mu/m$. In the case of bounded elliptic-like motion, one can prove [83] that the function $\mathcal{R}$ admits two real roots, $r_{\rm P} < r_{\rm A}$, which admit some non-zero finite Newtonian limits when $c \to \infty$, and represent respectively the radii of the orbit's periastron and apastron. The other roots tend to zero when $c \to \infty$.

We are considering a fixed binary's orbital configuration, fully specified by some given values of the integrals of motion E and J. We no longer indicate the dependence on E and J which is always implicit in what follows. The binary's orbital period, or time of return to the periastron, is obtained by integrating the radial motion as

$$P = 2\int_{r_{\rm P}}^{r_{\rm A}} \frac{dr}{\sqrt{\mathcal{R}[r]}}. \tag{3.5}$$

We introduce the fractional angle (*i.e.* divided by 2π) of the advance of the periastron per orbital revolution,

$$K = \frac{1}{\pi}\int_{r_{\rm P}}^{r_{\rm A}} dr \frac{\mathcal{G}[r]}{\sqrt{\mathcal{R}[r]}}. \tag{3.6}$$

which is such that the precession of the periastron per period is $\Delta\phi = 2\pi(K-1)$. As K tends to one in the limit $c \to \infty$ (as is easily checked from the Newtonian limits), it is convenient to pose $k \equiv K - 1$, which will then entirely describe the ***relativistic precession.***

Let us define the mean anomaly ℓ and the mean motion n by

$$\ell = n(t - t_{\rm P}), \tag{3.7a}$$

$$n = \frac{2\pi}{P}. \tag{3.7b}$$

$t_{\rm P}$ denotes the instant of passage to the periastron. For a given value of the mean anomaly ℓ the orbital separation r is obtained by inversion of the integral equation

$$\ell = n\int_{r_{\rm P}}^{r} \frac{d\rho}{\sqrt{\mathcal{R}[\rho]}}, \tag{3.8}$$

which defines the function $r(\ell)$ which is a periodic function in ℓ with period 2π. The orbital phase ϕ is obtained in terms of the mean anomaly ℓ by integrating the angular motion as

$$\phi = \phi_{\rm P} + \frac{1}{n}\int_0^{\ell} d\lambda' \, \mathcal{G}[r(\lambda')], \tag{3.9}$$

where $\phi_{\rm P}$ denotes the value of the phase at the instant $t_{\rm P}$. In the particular case of a circular orbit, $r = \text{const}$, the phase evolves linearly with time, $\dot{\phi} = \mathcal{G}[r] = \omega$, where ω is the orbital

frequency of the circular orbit given by

$$\omega = Kn = (1 + k)n. \tag{3.10}$$

In the general case of a non-circular orbit it is convenient to explicitly introduce the linearly growing part of the orbital phase 3.9 by writing it in the form

$$\phi = \phi_{\rm P} + \omega(t - t_{\rm P}) + W. \tag{3.11}$$

Here W denotes a certain function which is periodic in time with period P. Hence we can write the phase as

$$\phi = \phi_{\rm P} + K\ell + W, \tag{3.12}$$

where according to 3.9 the function W is given in terms of the mean anomaly ℓ by

$$W = \frac{1}{n}\int_0^{\ell} d\lambda' \left[\mathcal{G}\left[r(\lambda')\right] - \omega\right]. \tag{3.13}$$

The function $W(\ell)$ is a periodic function in ℓ. Finally the decomposition 3.12 exhibits clearly the doubly periodic nature of the binary motion, in terms of the mean anomaly ℓ with period 2π, and in terms of the periastron advance K t with period $2\pi K$. It may be noted that in Refs. [115, 47] the notation λ is used. It corresponds to $\lambda = {\rm K\,t}$ here.

3.3.2 Quasi-Keplerian representation of the motion

In the following we shall also use the explicit solution of the motion at 1PN order, in the form due to Damour and Deruelle [147, 171]. Then r and ℓ are expressed in terms of the eccentric anomaly u as

$$\mathrm{r} = a_r(1 - e_r \cos \mathrm{u}), \tag{3.14a}$$

$$\ell = u - e_t \sin u. \tag{3.14b}$$

The phase angle ϕ is given by

$$\phi = KV, \tag{3.15}$$

where as mentioned in the last chapter the true anomaly V is defined by,

$$V = 2\arctan\left[\left(\frac{1 + e_\phi}{1 - e_\phi}\right)^{1/2} \tan\frac{u}{2}\right]. \tag{3.16}$$

In the above, K is the periastron advance given in general terms in Eq. 3.6. The possible

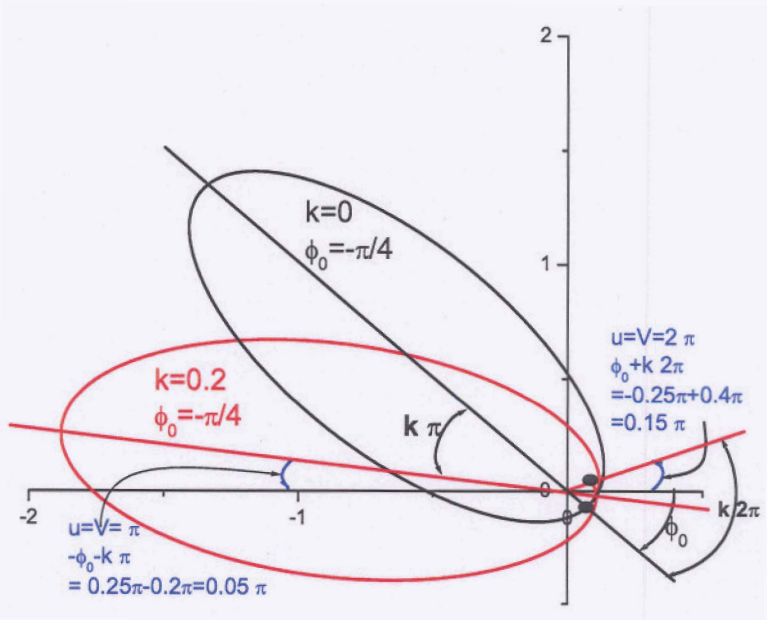

Figure 3.1: Plot showing a closed but non-precessing ($k = 0$) orbit and an orbit that is closed but precessing($k = 0.2$). Each orbit has an eccentricity of $e = 0.9$.

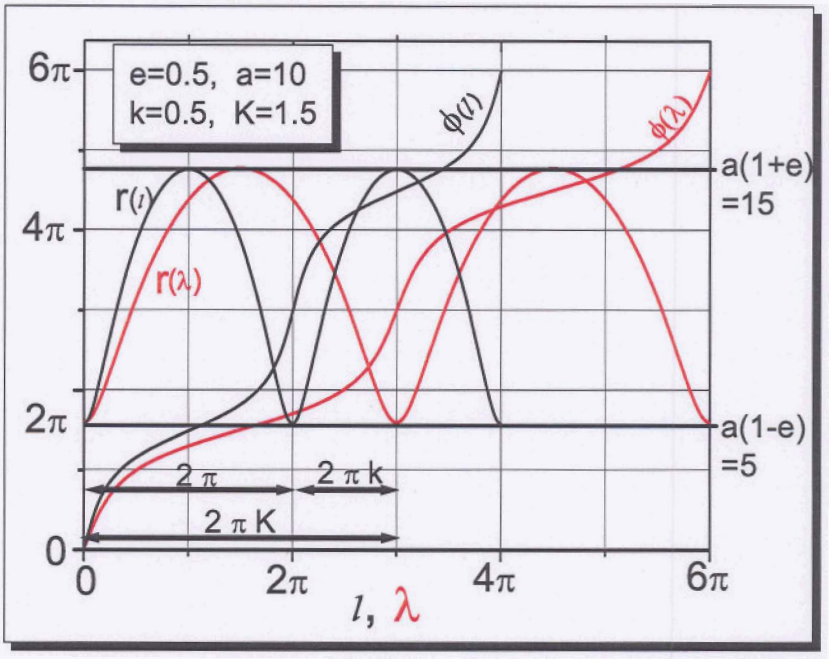

Figure 3.2: The plot illustrates the double periodicity. $r(l)$, $r(\lambda)$, $\phi(l)$ and $\phi(\lambda)$ are plotted respectively for an orbit with semimajor $a = 10$ and eccentricity $e = 0.5$. Here r is the length of the position vector measured from the focus. $a(1 + e) = 15$ and $a(1 - e) = 5$ are the maximum and minimum values of r. It is clear from the figure that $r(l)$ and $\phi(l)$ are 2π-periodic functions where as $r(\lambda)$ and $\phi(\lambda)$ are $2\pi K = 3\pi$-periodic functions. In this case the orbit is closed. The angular variable ϕ repeats after two periods of the radial variable.

additive constant in the equation for ϕ is set equal to zero. As mentioned in the last chapter, there are at 1PN order three kinds of eccentricities e_r, e_t and e_ϕ (labelled after the coordinates r, t and ϕ repectively) which differ from one another by 1PN terms. The advance of the periastron per orbital revolution appears starting at the 1PN order. Due to these features this representation is referred to as the "quasi-Keplerian"(QK) parametrization for the 1PN orbital motion of the binary. The periodic function $W(\ell)$ of **Eq.** 3.13 now reads

$$W = K\,(V - \ell)\ . \tag{3.17}$$

The explicit dependence of the orbital elements in terms of the 1PN conserved orbital energy E and angular momentum J is given in [147].

$$a, = \frac{1}{Gm}\frac{1}{(-2E)}\left\{1 + \frac{(-2E)}{4c^2}(-7+\nu)\right\}, \tag{3.18a}$$

$$e_r{}^2 = 1 + 2Eh^2 + \frac{(-2E)}{4c^2}\left\{24 - 4\nu + 5\,(-3+\nu)(-2Eh^2)\right\}, \tag{3.18b}$$

$$n = (-2E)^{3/2}\left\{1 + \frac{(-2E)}{8c^2}\,(-15+\mathrm{v})\right), \tag{3.18c}$$

$$e_t{}^2 = 1 + 2Eh^2 + \frac{(-2E)}{4c^2}\left\{-8 + 8\nu - (-17+7\nu)(-2Eh^2)\right\}, \tag{3.18d}$$

$$e_\phi{}^2 = 1 + 2Eh^2 + \frac{(-2E)}{4c^2}\left\{24 + (-15+\nu)(-2Eh^2)\right\}. \tag{3.18e}$$

In Figure 3.3.2 we plot the orbits for different values of e and k to give a schematic and physical feel for the double periodicity.

3.4 Fourier decomposition of the binary's multipole moments

The multipole moments of the compact binary system will be denoted by $I_L(t)$ (mass-type moment) and $J_L(t)$ (current-type), where the multi-index $\mathrm{L} = i_1 i_2 \cdots i_l$, with l being the multipolarity. We are adopting the same definitions of the post-Newtonian source moments as [98]. The general structure of these mass and current moments, I_L and say J_{L-1} (where $\mathrm{L}-1$ is taken rather than L for convenience), at any post-Newtonian order for a binary system moving on a general non-circular orbit is of the type

$$I_L(t) = \sum_{p=0} \mathcal{F}_p[r, \dot{r}^2, v^2]\, x^{<i_1\cdots i_p} v^{i_{p+1}\cdots i_l>}, \tag{3.19a}$$

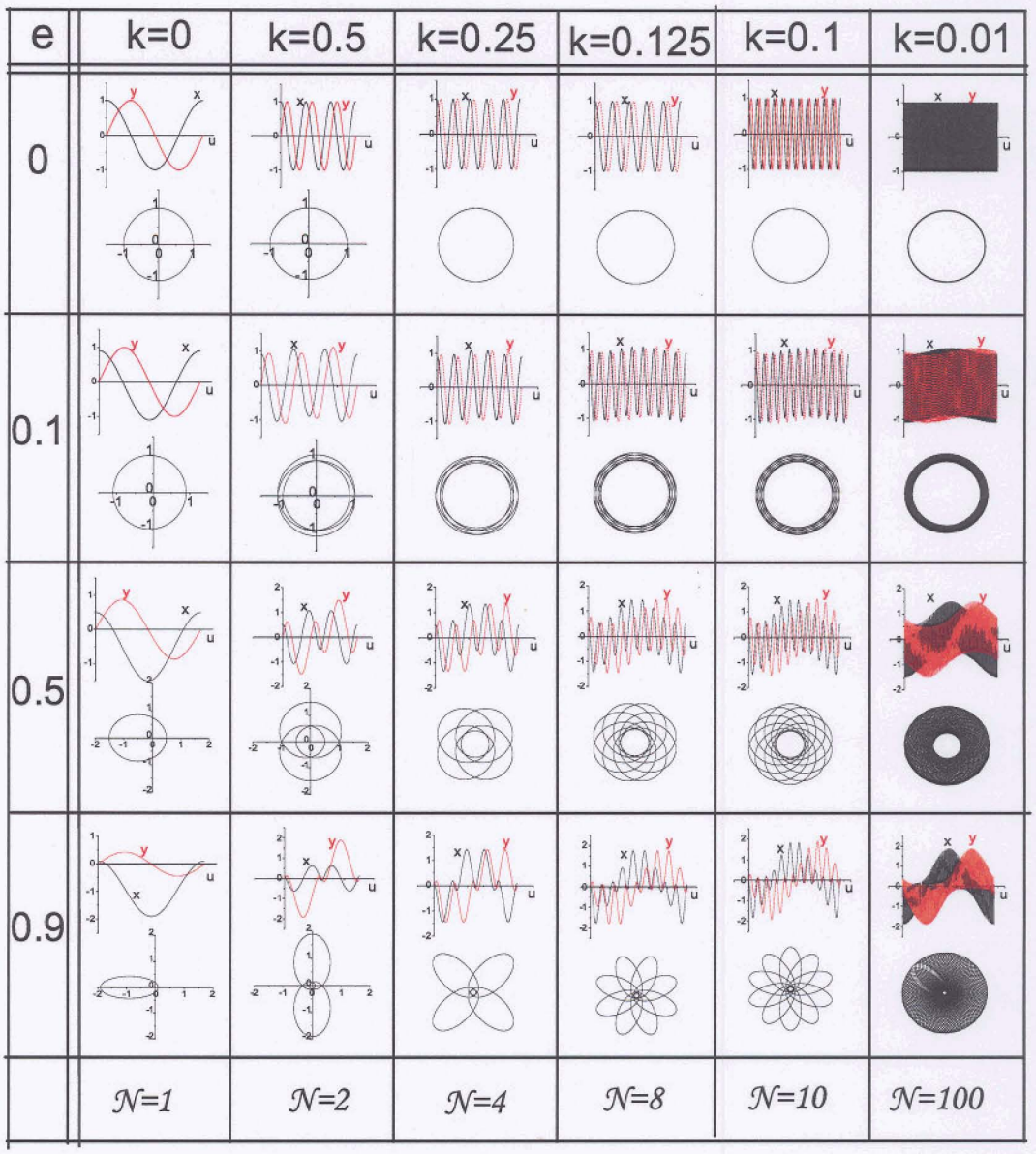

Figure 3.3: **Plot showing the variety** of closed orbits generated for different **combinations** of eccentricity e **and periastron shift** *k*. **The angular variable** ϕ **repeats after** N **periods** of the **radial variable (the** number of unclosed orbits before **coming** back **to the** *starting* **point). Note** $N = 1/k$ **for** $k \neq 0$.

$$J_{L-1}(t) = \sum_{p=0}^{l-2} \mathcal{G}_p[r, \dot{r}^2, v^2]\, x^{<i_1 \cdots i_p} v^{i_{p+1} \cdots i_{l-2}} \varepsilon^{i_{l-1}>ab} x^a v^b, \tag{3.19b}$$

where x^i and v^i are the relative position and velocity of the two bodies, and the coefficients $\mathcal{F}_p$ and $\mathcal{G}_p$ depend on r, $\dot{r}^2$ and $v^2 = \dot{r}^2 + r^2\dot{\phi}^2$. For quasi-elliptic motion in a plane, inserting $x = r\cos\phi$, $y = r\sin\phi$, and $v_x = \dot{r}\cos\phi - r\dot{\phi}\sin\phi$, $v_y = \dot{r}\sin\phi + r\dot{\phi}\cos\phi$, we can explicitly factorize out the dependence on the orbital phase ϕ. Furthermore, using the explicit solution of the motion (Sec. 3.3) we can express r, $\dot{r}^2$ and v^2, and hence the $\mathcal{F}_p$'s and $\mathcal{G}_p$'s, as periodic function of the mean anomaly $\ell = n(t - t_0)$, where $n = 2\pi/P$. We then find the general structure can be expressed in terms of the phase angle ϕ, as the following finite sum over an index m ranging from $-l$ to +1,

$$I_L(t) = \sum_{m=-l}^{l} {}_{(m)}\mathcal{A}_L(\ell)\, e^{im\phi}, \tag{3.20a}$$

$$J_{L-1}(t) = \sum_{m=-l}^{l} {}_{(m)}\mathcal{B}_{L-1}(\ell)\, e^{im\phi}, \tag{3.20b}$$

with some complex coefficients ${}_{(m)}\mathcal{A}_L$ and ${}_{(m)}\mathcal{B}_{L-1}$. The important point for our purpose is that the functions ${}_{(m)}\mathcal{A}_L(\ell)$ and ${}_{(m)}\mathcal{B}_{L-1}(\ell)$ are now 2π-periodic functions of ℓ. As we can see, the structure of the mass and current moments is the same, but of course the coefficients ${}_{(m)}\mathcal{A}_L$ and ${}_{(m)}\mathcal{B}_{L-1}$ have a different parity, because of the Levi-Civita symbol ε^{iab} entering the current moment.

In the above expressions, the variable ϕ is not a periodic function of ℓ. To proceed further, we need to exploit the double periodicity of the dynamics in the two variables $\lambda = Kt$ and ℓ by writing, $\phi = Kt + W(\ell)$, where $W(\ell)$ is periodic in ℓ; see Sec. 3.3. Actually it will be more convenient to single out in the expression of the phase the purely relativistic precession of the periastron kt, where $k = K - 1$. This yields many factors which will modify the coefficients in 3.20a, but in such a way that they remain periodic in ℓ. Hence we can write

$$I_L(t) = \sum_{m=-l}^{l} {}_{(m)}\mathcal{I}_L(\ell)\, e^{imk\ell}, \tag{3.21a}$$

$$J_{L-1}(t) = \sum_{m=-l}^{l} {}_{(m)}\mathcal{J}_{L-1}(\ell)\, e^{imk\ell}. \tag{3.21b}$$

Finally this makes it possible to use a Fourier series expansion in the interval $[0, 2\pi]$ for each

of the functions in 3.21, leading then to the following discrete Fourier decompositions,

$$I_L(t) = \sum_{p=-\infty}^{+\infty} \sum_{m=-l}^{l} \underset{(p,m)}{\mathcal{I}}_L e^{i(p+mk)\ell}, \tag{3.22a}$$

$$J_{L-1}(t) = \sum_{p=-\infty}^{+\infty} \sum_{m=-l}^{l} \underset{(p,m)}{\mathcal{J}}_{L-1} e^{i(p+mk)\ell}. \tag{3.22b}$$

Since the moments I_L and J_{L-1} are real we have obviously ${}_{(p,m)}\mathcal{I}^*_L = {}_{(-p,-m)}\mathcal{I}_L$ and ${}_{(p,m)}\mathcal{J}^*_{L-1} = {}_{(-p,-m)}\mathcal{J}_{L-1}$.

At the Newtonian order (hence in the limit where k $\to$ ***0),*** we recover the usual periodic Fourier decomposition of the moments, with only one discrete Fourier summation index p, by writing

$$I_L(t) = \sum_{p=-\infty}^{+\infty} \underset{(p)}{\mathcal{I}}_L e^{ip\ell}, \tag{3.23a}$$

$$J_{L-1}(t) = \sum_{p=-\infty}^{+\infty} \underset{(p)}{\mathcal{J}}_{L-1} e^{ipt}. \tag{3.23b}$$

These Fourier coefficients are simply equal to the sums over m of the doubly-periodic Fourier coefficients in Eqs. 3.22, when taken in this Newtonian limit,

$$\underset{(p)}{\mathcal{I}}_L = \sum_{m=-l}^{l} \underset{(p,m)}{\mathcal{I}}_L, \tag{3.24a}$$

$$\underset{(p)}{\mathcal{J}}_{L-1} = \sum_{m=-l}^{l} \underset{(p,m)}{\mathcal{J}}_{L-1}. \tag{3.24b}$$

3.5 Tail contributions in the flux of compact binaries

In the present Section we compute all the tail and tail-of-tail terms in the averaged gravitational-wave energy flux

$$\mathcal{F} \equiv -\left(\frac{d\mathcal{E}}{dt}\right)^{\rm GW} \equiv -\left\langle\left(\int d\Omega \, \frac{d\mathcal{E}}{dt\, d\Omega}\right)\right\rangle^{\rm GW}, \tag{3.25}$$

up to the 3PN order. The relevant expressions are given in Eq. 3.1. Together with the instantaneous terms **Eq.** 2.7 in the previous chapter one obtains complete expressions of the 3PN energy flux.

3.5.1 The quadrupolar tail at Newtonian order

The mass-type quadrupolar tail term in the energy flux is made of a non-linear interaction between the quadrupole and the mass monopole, and is given by [1]

$$\mathcal{F}_{\text{mass quad}} = \langle \frac{4M}{5} I_{ij}^{(3)}(t) \int_0^{+\infty} d\tau \, I_{ij}^{(5)}(t-\tau)\left[\ln\left(\frac{\tau}{\tau_0}\right) + \frac{11}{12}\right]\rangle, \tag{3.26}$$

where I_{ij} is the source's mass-type quadrupole moment, and M its ADM mass. The brackets $\langle\rangle$ denote the average over ℓ, where the superscript (n) refers to time differentiations, and where TO is a constant time scale (related to the length scale r_0 appearing in the general multipolar formalism [98] by $\tau_0 = 2r_0/c$). The term was already computed using a Fourier series at Newtonian order in [145]; note that the method of [145] is applicable only at Newtonian order since it is valid only for periodic motion. Here we first recover the Newtonian result of [145]. The Fourier decomposition of the Newtonian quadrupole moment reads

$$I_{ij}(t) = \sum_{p=-\infty}^{+\infty} \underset{(p)}{I_{ij}} \, e^{ip\ell}, \tag{3.27}$$

and all the Fourier coefficients are at Newtonian order. We insert that decomposition into the flux 3.26. The average on ℓ is easily performed with the formula

$$\langle e^{ip\ell} \rangle \equiv \int_0^{2\pi} \frac{d\ell}{2\pi} \, e^{ip\ell} = \delta_{p,0}, \tag{3.28}$$

and we have used the fact that if $\ell(t)$ corresponds to the current time t, then it is clear that $\ell(t-\tau) = \ell(t) - n\tau$ corresponds to the retarded time $t - \tau$. The result is

$$\mathcal{F}_{\text{mass quad}} = -\frac{4M}{5} \sum_{p=-\infty}^{+\infty} (p\,n)^8 \, |\underset{(p)}{I_{ij}}|^2 \int_0^{+\infty} d\tau \, e^{ip\,n\tau}\left[\ln\left(\frac{\tau}{\tau_0}\right) + \frac{11}{12}\right]. \tag{3.29}$$

Finally the last factor in 3.29, namely the tail integral in the Fourier domain, is computed using the formula

$$\int_0^{+\infty} d\tau \, e^{i\sigma\tau} \ln\left(\frac{\tau}{\tau_0}\right) = -\frac{1}{\sigma}\left[\frac{\pi}{2}\text{sign}(\sigma) + i\Big(\ln(|\sigma|\tau_0) + C\Big)\right], \tag{3.30}$$

where $\sigma = \text{pn}$, $\text{sign}(\sigma) = \pm 1$ and $C = 0.577\cdots$ is Euler's constant. Inserting then the tail integral 3.30, we check that the imaginary parts cancel out, and the result reduces to the one

[1] For simplicity we do not indicate the neglected PN terms, *e.g.* $O(c^{-2})$. This sometimes yields some slight inconsistency in the notation, but the meaning of each equation should be clear from the context.

of [145], namely

$$\mathcal{F}_{\text{mass quad}} = \frac{4\pi M}{5}\sum_{p=1}^{+\infty}(p\,n)^7\,|\underset{(p)}{I}_{ij}|^2. \tag{3.31}$$

Unfortunately, the latter result has to be left in the form of an infinite series of Fourier components, since no analytic closed-form expression for it can be found.

We stress finally that the result 3.31 (and this applied as well to all results in this Section) is not exact. Indeed we have formally replaced inside the tail integral the motion of the binary at any earlier time $t-\tau$ by its motion at the current t, thereby neglecting the binary's evolution by radiation reaction. As a result there should be a remainder term in 3.34, given by the order of magnitude of the adiabatic parameter ξ_{rad} of the inspiral, which is related to the radiation reaction time scale, and is given by the rate of decrease of the orbital frequency due to gravitational radiation emission, say $\xi_{\text{rad}} = \dot{\omega}/\omega^2$. In terms of a PN expansion ξ_{rad} is a correction of relative 2.5PN order $\sim c^{-5}$. Indeed, we know (*e.g.* [145]) that the replacement of the current motion inside the tail integral is valid only in the adiabatic limit, modulo $O(\xi_{\text{rad}})$ terms.

3.5.2 The quadrupolar tail at 1PN order

Let us now tackle the same computation but at the 1PN order. At this order, as we have seen, we must exploit the doubly-periodic structure of the motion, and use a more general expression for the Fourier decomposition of the moments. The post-Newtonian quadrupole moment admits a structure of the type described in Sec. 3.4, namely

$$I_{ij}(t) = \sum_{p=-\infty}^{+\infty}\sum_{m=-2}^{2}\underset{(p,m)}{I}_{ij}\,e^{i(p+mk)\ell}, \tag{3.32}$$

but with now doubly-indexed Fourier coefficients $\underset{(p,m)}{I}_{ij}$ which now involve post-Newtonian corrections. We can even be more precise and notice that the harmonics for which m = 1 and m = −1 are in fact zero (at the 1PN order), so that

$$I_{ij}(t) = \sum_{p=-\infty}^{+\infty}\left\{\underset{(p,0)}{I}_{ij}\,e^{ip\ell} + \underset{(p,2)}{I}_{ij}\,e^{i(p+2k)\ell} + \underset{(p,-2)}{I}_{ij}\,e^{i(p-2k)\ell}\right\}. \tag{3.33}$$

However, it is more convenient in the following to work with the general decomposition 3.27, keeping in mind that the terms with m = 1 or −1 are absent. As before we insert the double Fourier series 3.27 into the expression of the flux 3.26. This readily yields, still in the

adiabatic limit, *i.e.* neglecting $O(\xi_{\rm rad})$ corrections,

$$\mathcal{F}_{\rm mass\ quad} = \frac{4M}{5}\sum_{p,p'\neq 0,m'} n^8(p+mk)^3(p'+m'k)^5\,\mathbf{I}^{ij}_{(p,m)}\,\mathbf{I}^{ij}_{(p',m')} \times\langle e^{i(p+p'+(m+m')k)\ell}\rangle\int_0^{+\infty} d\tau\, e^{-i(p'+m'k)n\tau}\left[\ln\left(\frac{\tau}{\tau_0}\right)+\frac{11}{12}\right]. \qquad (3.34)$$

The summations range from $-\infty$ to $+\infty$ for p and p', and from -2 to 2 for m and m'. The first two factors after the summation signs evidently come from the time-derivatives of the quadrupole moment. We have explicitly left as they are the last two factors which are the average over ℓ of an elementary doubly-periodic complex exponential, and the tail integral in the Fourier domain.

We want now to work out the expression **3.34** at the specific 1PN order. Since the relativistic advance of the periastron k is already a small quantity of order 1PN, the first thing to do is to evaluate **3.34** at first order in k [*i.e.*, neglecting $O(k^2)$]. Later we shall have to insert some explicit expression for the 1PN expansion of the components of the quadrupole moment itself. We provide here the necessary formulas for performing the expansion in k of the last two factors in **3.34.** For the E-average, which is defined by

$$\langle e^{i(p+mk)\ell}\rangle \equiv \int_0^{2\pi}\frac{d\ell}{2\pi}\,e^{i(p+mk)\ell}, \qquad (3.35)$$

we readily find the following result, using the fact that since we are in the limit where $k \to 0$ we shall always have $mk \ll 1$ (hence $\mathbf{p}+mk$ is never an integer except when $p=0$):

$$\langle e^{i(p+mk)\ell}\rangle = \left\{\begin{array}{ll}\dfrac{m}{p}k & \text{if } p\neq 0\\[2ex] 1+i\pi mk & \text{if } p=0\end{array}\right\} + O(k^2). \qquad (3.36)$$

We notice that this result depends only on whether p is zero or not, and is true for any integer m, with the small exception that when $m=0$ the result **3.36** is "exact" as there is no remainder term $O(k^2)$. Concerning the tail integral in **3.34,** we expand it at first order in k, obtaining

$$\int_0^{+\infty} d\tau\, e^{i(p+mk)n\tau}\ln\left(\frac{\tau}{\tau_0}\right) = \left(1-\frac{mk}{p}\right)\int_0^{+\infty} d\tau\, e^{ip\,n\tau}\ln\left(\frac{\tau}{\tau_0}\right) - i\frac{mk}{p^2 n} + O(k^2), \qquad (3.37)$$

and then apply for the remaining integral the formula **3.48.** With the formulas **3.36** and **3.37** in hand we can explicitly work out the tail expression **3.34** at first order in k (and the extension at higher order in k would in principle be straightforward). The result will be left in the form of some infinite series, directly obtained by replacing **3.36** and **3.48** into **3.34,**

that we shall compute numerically below as a function of the eccentricity.

3.5.3 Higher-order multipolar tails

In our calculation of the binary's fluxes at 3PN order, the only tail integral which has to be computed at relative 1PN order is the quadratic tail integral discussed in the previous subsection. All other tails, and tails-of-tails, can be computed at the (relative) Newtonian order. We compute here the relevant multipolar tails. Their definitions are [95]

$$\mathcal{F}_{\text{mass oct}} = \langle \frac{4\mathrm{M}}{189} I^{(4)}_{ijk}(t) \int_0^{+w} d\tau\, I^{(6)}_{ijk}(t-\tau)\Big[\ln\Big(\frac{\tau}{\tau_0}\Big) + \frac{97}{60}\Big]\rangle, \tag{3.38}$$

$$\mathcal{F}_{\text{mass dodec}} = \langle \frac{\mathrm{M}}{2268} I^{(5)}_{ijkl}(t) \int_0^{+w} d\tau\, I^{(7)}_{ijkl}(t-\tau)\Big[\ln\Big(\frac{\tau}{\tau_0}\Big) + \frac{59}{30}\Big]\rangle, \tag{3.39}$$

in the case of mass-type multipolar tails, and

$$\mathcal{F}_{\text{curr quad}} = \langle \frac{64M}{45} J^{(3)}_{ij}(t) \int_0^{+\infty} d\tau\, J^{(5)}_{ij}(t-\tau)\Big[\ln\Big(\frac{\tau}{\tau_0}\Big) + \frac{7}{6}\Big]\rangle, \tag{3.40}$$

$$\mathcal{F}_{\text{curr oct}} = \langle \frac{M}{21} J^{(4)}_{ijk}(t) \int_0^{+\infty} d\tau\, J^{(6)}_{ijk}(t-\tau)\Big[\ln\Big(\frac{\tau}{\tau_0}\Big) + \frac{5}{3}\Big]\rangle, \tag{3.41}$$

for the current-type ones. The computation proceeds exactly as for the Newtonian quadrupole tail in Sec. 3.5.1, and we give only the results:

$$\mathcal{F}_{\text{mass oct}} = \frac{4\pi M}{189} \sum_{p=1} (p\,n)^9 \,|\mathcal{I}_{ijk}|^2, \tag{3.42}$$

$$\mathcal{F}_{\text{mass dodec}} = \frac{\pi M}{2268} \sum_{p=1}^{+\infty} (p\,n)^{11} \,|\mathcal{I}_{ijkl}|^2, \tag{3.43}$$

$$\text{quad} = \frac{64\pi\mathrm{M}}{45} \sum_{p=1}^{+\infty} (p\,n)^7 \,|\mathcal{J}_{ij}|^2, \tag{3.44}$$

$$\mathcal{F}_{\text{curr oct}} = \frac{\pi M}{21} \sum_{p=1}^{+\infty} (p\,n)^7 \,|\mathcal{J}_{ijk}|^2. \tag{3.45}$$

As we see, these results can be expressed in terms of rather simple Fourier series, unlike in the case of the 1PN quadrupole tail 3.34 which is substantially more intricate when the summations are fully explicated. As in [145] we shall provide some numerical plots for these results, since the infinite sums 3.42 cannot be computed analytically.

3.5.4 Quadrupolar tail-of-tail and tail squared

At the 3PN order (*i.e.* 1.5PN beyond the dominant tail) appear the first tail-of-tail as well as a term composed of the square of the tail, both of them being made of interactions between the quadrupole and the mass [158]. The tail-of-tail contribution admits the expression

$$\mathcal{F}_{\text{quad tail(tail)}} = \langle \frac{4M^2}{5} I_{ij}^{(3)}(t) \int_0^{+\infty} d\tau\, I_{ij}^{(6)}(t-\tau)\left[\ln^2\left(\frac{\tau}{\tau_0}\right) + \frac{57}{70}\ln\left(\frac{\tau}{\tau_0}\right) + \frac{124627}{44100}\right]\rangle, \quad (3.46)$$

while the tail squared one is

$$\mathcal{F}_{\text{quad (tail)}^2} = \langle \frac{4M^2}{5}\left(\int_0^{+\infty} d\tau\, I_{ij}^{(5)}(t-\tau)\left[\ln\left(\frac{\tau}{\tau_0}\right) + \frac{11}{12}\right]\right)^2\rangle. \quad (3.47)$$

As before we insert into these the Fourier decomposition of the quadrupole moment 3.27. The new feature with respect to previous computations is of course the occurence of a term with a logarithm squared in the tail-of-tail integral 3.46. The corresponding formula necessary to compute this logarithm squared is [compare with Eq. 3.481

$$\int_0^{+\infty} d\tau\, e^{i\sigma\tau} \ln^2\left(\frac{\tau}{\tau_0}\right) = \frac{i}{\sigma}\left\{\frac{\pi^2}{6} - \left[\frac{\pi}{2}\text{sign}(\sigma) + i\left(\ln(|\sigma|\tau_0) + C\right)\right]^2\right\}. \quad (3.48)$$

With this formula together with 3.48 we obtain for the tail-of-tail

$$\mathcal{F}_{\text{quad tail(tail)}} = \frac{4M^2}{5}\sum_{p=1}^{+\infty}(pn)^8 |I_{(p)ij}|^2 \left\{\frac{\pi^2}{6} - 2\left(\ln(pn\tau_0) + C\right)^2 + \frac{57}{35}\left(\ln(pn\tau_0) + C\right) - \frac{124627}{22050}\right\}, \quad (3.49)$$

and also, for the tail squared,

$$\text{quad (tail)}^2 = \frac{4M^2}{5}\sum_{p=1}^{+\infty}(pn)^8 |I_{(p)ij}|^2 \left\{\frac{\pi^2}{2} + 2\left(\ln(pn\tau_0) + C - \frac{11}{12}\right)^2\right\}. \quad (3.50)$$

As we can see the contribution from logarithms squared cancel each other between 3.49 and 3.50, see [158], and we finally get

$$\text{quad tail(tail)+(tail)}^2 = \frac{4M^2}{5}\sum_{p=1}^{+\infty}(pn)^8 |I_{(p)ij}|^2 \left\{-\frac{116761}{29400} + \frac{2n^2}{3} - \frac{214}{105}C - \frac{214}{105}\ln(pn\tau_0)\right\}. \quad (3.51)$$

3.6 Definition of the eccentricity enhancement factors

We define here some functions of the eccentricity by certain Fourier series of the components of the Newtonian moments $I_L = \mu x^{<L>}$ and $J_{L-1} = \mu x^{<L-2}\varepsilon^{i_{l-1}>ab} x^a v^b$ for a Keplerian ellipse with semi-major axis a, eccentricity e and frequency $n = 2\pi/P$. We rescale the moments to adimensionalize them by defining

$$\hat{I}_L \equiv \frac{I_L}{\mu a^l}, \tag{3.52a}$$

$$\hat{J}_{L-1} \equiv \frac{J_{L-1}}{\mu a^l n}. \tag{3.52b}$$

Then we define the some dimensionless Fourier series, which are functions only of the (Keplerian) eccentricity e. First of all the function

$$f(e) = \frac{1}{16}\sum_{p=1}^{+\infty} p^6 |\hat{I}_{(p)ij}|^2, \tag{3.53}$$

is nothing but the Peters & Mathews "enhancement" function [138], which enters the energy flux at the Newtonian order (given by the Einstein quadrupole formula), *i.e.*

$$\mathcal{F}_{\rm N} = \frac{32}{5}\nu^2 x^5 f(e), \tag{3.54}$$

when computed using Fourier series. Remarkably f (e) admits an algebraically closed-form expression, crucial for the timing of the binary pulsar PSR 1913+16, and given by

$$f(e) = \frac{1 + \frac{73}{24}e^2 + \frac{37}{96}e^4}{(1-e^2)^{7/2}}. \tag{3.55}$$

The enhancement function $f(e)$ is called that way because in the case of the binary pulsar, which has eccentricity e = 0.617... it enhances the effect of the orbital P by a factor ~ 11.843.

Next we define several other eccentricity "enhancement" functions which constitute useful ingredients when parametrizing the tail terms at Newtonian order. We pose

$$\varphi(e) = \frac{1}{32}\sum_{p=1}^{+\infty} p^7 |\hat{I}_{(p)ij}|^2, \tag{3.56}$$

$$\beta(e) = \frac{20}{49209}\sum_{p=1}^{+\infty} p^9 |\hat{I}_{(p)ijk}|^2, \tag{3.57}$$

$$\gamma(e) = 4\sum_{p=1}^{+\infty} p^7 |\hat{\mathcal{J}}_{ij}|^2. \tag{3.58}$$

Like for f (e) these functions are defined in such a way that they tend to one in the circular orbit limit, when e → 0. However, unlike for f (e), they do not admit closed-form expressions, and must be left in the form of Fourier series. The function $\varphi(e)$ has already been computed numerically in [145][2]. With their help the Newtonian tail terms computed in Sec. 3.5 read

$$\mathcal{F}_{\text{mass quad}} = \frac{32}{5} \mathrm{v}^2 x^{13/2} \left\{ 4\pi \varphi(e) \right\}, \tag{3.59}$$

$$\mathcal{F}_{\text{mass oct}} = \frac{32}{5} \mathrm{v}^2 x^{15/2} \left\{ \frac{16403}{2016} \pi \beta(e) \right\} (1 - 4\nu), \tag{3.60}$$

$$\mathcal{F}_{\text{curr quad}} = \frac{32}{5} \mathrm{v}^2 x^{15/2} \left\{ \frac{1}{18} \pi \gamma(e) \right\} (1 - 4\,\mathrm{v}), \tag{3.61}$$

where we have factorized out a coefficient appropriate to the Newtonian expression of the flux for circular orbits; compare with Eq. 3.54.

Next we introduce two other enhancement functions which are helpful when parametrizing the tail-of-tail and tail squared integrals (which we recall are Newtonian with the present approximation). Namely

$$F(e) = \frac{1}{64}\sum_{p=1}^{+\infty} p^8 |\hat{I}_{(p)ij}|^2, \tag{3.62}$$

$$\chi(e) = \frac{1}{64}\sum_{p=1}^{+\infty} p^8 \ln\left(\frac{p}{2}\right) |\hat{I}_{(p)ij}|^2. \tag{3.63}$$

It is easily checked, by a straightforward calculation *à la* Peters & Mathews [138], that the function $F(e)$ admits an analytic form similar to the one of f (e) and given by

$$F(e) = \frac{1 + \frac{85}{6}e^2 + \frac{5171}{192}e^4 + \frac{1751}{192}e^6 + \frac{297}{1024}e^8}{(1 - e^2)^{13/2}} \tag{3.64}$$

On the other hand, $\chi(e)$ does not admit any analytic form, but is easily seen to tend to zero when e → 0. Indeed, at Newtonian order and in the circular orbit limit, the quadrupole moment admits only one harmonic, which is the one for which p = 2. But, because of the logarithmic term in $\chi(e)$, we see that the function is zero when e = 0.

Now, in terms of $F(e)$ and $\chi(e)$, the sum of tail-of-tail and tail squared contributions

[2]Note that our notation here is different from the one in [145]; the function $\varphi^{\text{BS}}(e)$ there is related to our definition by $\varphi^{\text{BS}}(e) = \varphi(e)/\mathrm{f}$ (e). In the present work it is better to not rescale the various functions using the Peters & Mathews "enhancement" function f (e).

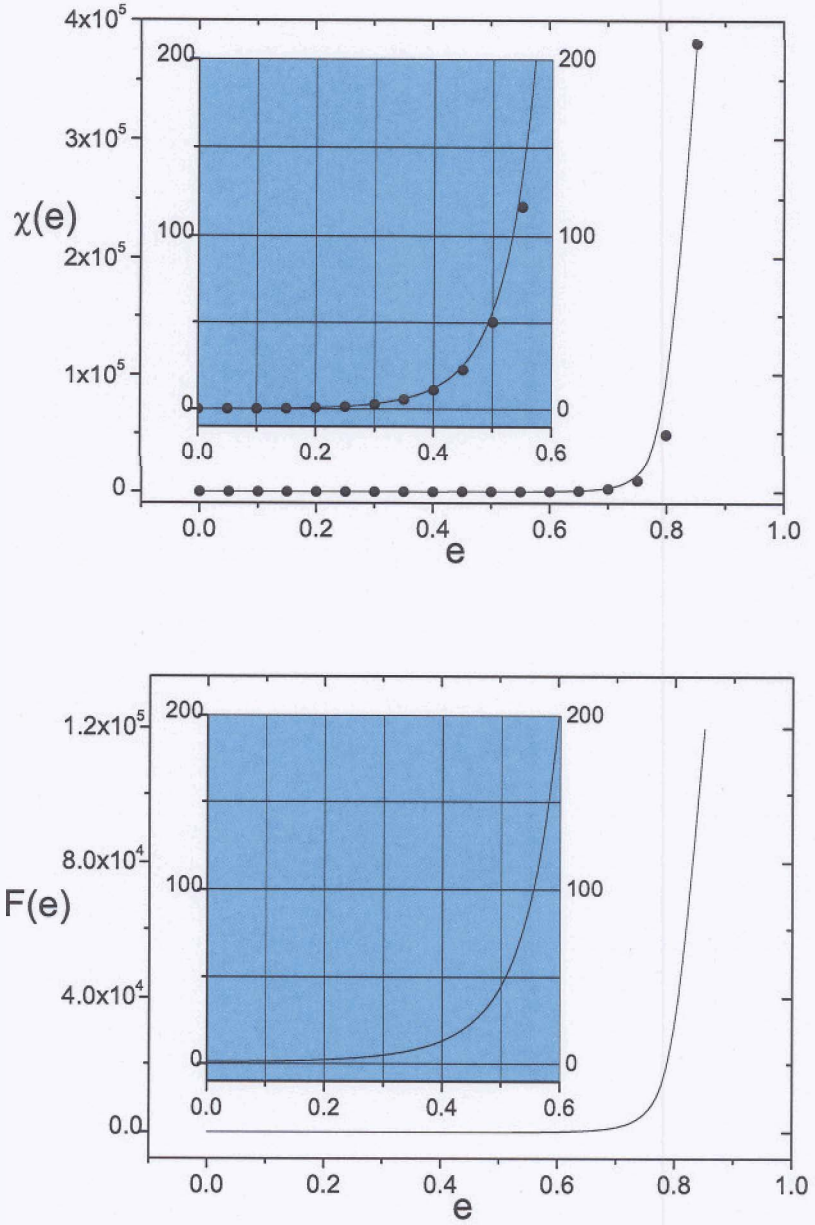

Figure 3.4: This figure shows the variation **of** $\chi(e_t)$ **(top panel) and** $F(e_t)$ (bottom **panel) with** the **eccentricity** e_t. **The** plot **inside** the **graph is the** zooming **for** the functions **which look as** straight horizontal **lines in main graph. In the top panel the** dot **points are the numerical** computation for $\chi(e_t)$ **at** $e_t = 0, 0.5, 1, 1.5, \ldots$ **The** solid **lines are the fitting for the** numerical **points. In the** bottom **panel, the exact** function **of** $F(e_t)$ **is used. At** the **circular** limit, $e_t = 0$, $\chi(0) = 0$, $F(0) = 1$.

computed in Sec. 3.5 reads

$$\mathcal{F}_{\text{tail(tail)+(tail)}^2} = \frac{32}{5}\nu^2 x^8\left\{\left[-\frac{116761}{3675}+\frac{16}{3}\pi^2-\frac{1712}{105}C-\frac{1712}{105}\ln\left(\frac{4\omega r_0}{c}\right)\right]F(e)-\frac{1712}{105}\chi(e)\right\}. \tag{3.65}$$

Finally let us give the result in the case of the 1PN quadrupole tail. As we have seen in Sec. 3.5.2, the calculation in this case is much more complicated, as the Fourier series in Eq. 3.34 involve several summations. In addition the computation must take into account the 1PN relativistic correction in the quadrupole moment (and ADM mass). There is no simple way to express the new "enhancement" functions of eccentricity which appear at the 1PN order. However one can check beforehand that the 1PN terms are a linear function of the symmetric mass ratio v, hence we must introduce two enhancement functions, denoted a and 8, and as previously we define them in such a way that they are equal to one for circular orbits. We shall therefore give here only the definition of these functions, and resort to a numerical calculation of them in the next Section. We have [extending Eq. 3.9 at the 1PN order]

$$\mathcal{F}_{\text{mass quad}} = \frac{32}{5}\nu^2 x^{13/2}\left\{4\pi\,\varphi(e_t)+\pi\,\text{x}\left[-\frac{428}{21}\alpha(e_t)+\frac{178}{21}\nu\,\theta(e_t)\right]\right\}. \tag{3.66}$$

Note that since we are at 1PN order we must use a specific definition for the eccentricity, and we adopted the eccentricity e, defined in Sec. 3.3.2. On the other hand, the variable $\text{x} = (m\omega)^{2/3}$ crucially incorporates the 1PN relativistic correction coming from the periastron advance $K = 1 + \text{k}$, through the definition $\omega = nK$; see Sec. 3.3.1.

3.7 Numerical evaluation of the Fourier coefficients

We shall now describe the numerical implementation of the procedure for computation of the Fourier coefficients of the multipole moments, notably the ${}_{(p,m)}I_{ij}$'s at 1PN order which are the more difficult to obtain. The mass quadrupole moment to 1PN accuracy is given by:

$$\begin{aligned} I_{ij} = {} & \nu m\left\{1+\frac{1}{c^2}\left[v^2\left(\frac{29}{42}-\frac{29\nu}{14}\right)+\frac{Gm}{r}\left(-\frac{5}{7}+\frac{8}{7}\nu\right)\right]x_{\langle i}x_{j\rangle}\right. \\ & \left.+\left(\frac{11}{21}-\frac{11}{7}\right)\frac{r^2}{c^2}v_{\langle i}v_{j\rangle}+2\left(-\frac{2}{7}+\frac{6}{7}\right)\frac{r\dot{r}}{c^2}x_{\langle i}v_{j\rangle}\right\}. \end{aligned} \tag{3.67}$$

We also will need the ADM mass M to 1PN accuracy:

$$M = m\left[1+\frac{\nu}{c^2}\left(\frac{v^2}{2}-\frac{Gm}{r}\right)+O(4)\right]. \tag{3.68}$$

Using the quasi-Keplerian representation, the dependence of I_{ij} on xi, v_i, r, v and $\dot{r}$ can be parametrised in terms of of th eccentric anomaly u. However, as explained previously we require $I_{ij}(\ell)$ in the time domain to proceed

The steps of our numerical implementation scheme can be now summarised as follows.

1. We first invert the equation for the mean anomaly $\ell = u - e_t \sin u$ to obtain $u(\ell)$. This can be done

   - By using
   $$u = \ell + 2\sum_{1}^{\infty} \frac{1}{s} J_s(se) \sin s\ell, \tag{3.69}$$
   - Or mumerically by finding the root of $\ell = u - e_t \sin u$ to obtain $u(\ell)$.

   The latter is a more efficient and more accurate method and we employ it in this work. We used the FindRoot routine in Mathematica. In this case we generated a table of 20000 points of u and ℓ between 0 and 2π. The above inversion enables us to re-express all functions of the eccentric anomaly u as functions of the mean anomaly ℓ. One needs to be careful in dealing with the u dependence of V in Eq. 3.16 to avoid the discontinuity there. To this end it is best to use:
   $$V(u) = u + 2\tan^{-1}\left(\frac{\beta_\phi \sin u}{1 - \beta_\phi \cos u}\right), \tag{3.70}$$
   where $\beta_\phi = \frac{1-\sqrt{1-e_\phi^2}}{e_\phi}$. With these choices, we thus have on hand, ${}_{(m)}\mathcal{I}_{ij}(\ell)$ [defined in Eq. 3.211 as explicit functions of ℓ to implement the Fourier decomposition.

2. Recall that these functions also have dependence on v and x, where the former is the symmetric mass ratio and the latter the PN parameter given by $x = (m\omega)^{2/3}$ with $\omega = n K$. To avoid assuming numerical values for v and x and hence to preserve the full generality of the result, we split the function ${}_{(m)}\mathcal{I}_{ij}$ as
   $$\underset{(m)}{\mathcal{I}}_{ij}(\ell, e_t, \nu, x) = \underset{(m)}{\mathcal{I}}{}^{00}_{ij}(\ell, e_t) + x\left[\underset{(m)}{\mathcal{I}}{}^{10}_{ij}(\ell, e_t) + \nu\,\underset{(m)}{\mathcal{I}}{}^{11}_{ij}(\ell, e_t)\right]. \tag{3.71}$$
   Notice that we have neglected the terms higher than 1PN in writing down the above expression. Now the various ${}_{(m)}\mathcal{I}^{ab}_{ij}$ are only function of ℓ and e_t. We evaluate the Fourier coefficients of these terms separately in the next step of the procedure.

3. For a fixed value of e_t, we can straightforwardly get the plot of ${}_{(m)}\mathcal{I}^{00}_{ij}$ versus C. Equiv-

alently, one can also write the Fourier decomposition of ${}_{(m)}\mathcal{I}_{ij}^{00}(\ell)$ as

$$\mathcal{I}_{ij}^{00}(\ell) = \sum_{p=-\infty}^{+\infty} \underset{(p,m)}{\mathcal{I}_{ij}^{00}} e^{ip\ell}. \tag{3.72}$$

Now we seek a numerical fit to Eq. (3.71), in powers of $e^{ip\ell}$, to extract out the coefficients ${}_{(p,m)}\mathcal{I}_{ij}^{00}$. Do the same for different values of e_t and for ${}_{(p,m)}\mathcal{I}_{ij}^{10}$ and ${}_{(p,m)}\mathcal{I}_{ij}^{11}$.

4. Substituting these values into Eq. 3.34 one can generate the numerical values of the averaged energy flux $\mathcal{F}_{\text{tail}}$ for the different values of e_t, and hence get the numerical values of the enhancement functions, and most importantly of the 1PN ones $\alpha(e_t)$ and $\theta(e_t)$. The plots of the functions as given in Eq. 3.92 readily follow.

We have just described the procedure for the most difficult 1PN quadrupole tail. This procedure is quite general, and could be extended to higher post-Newtonian orders. On the other hand, for the other tail terms, which are Newtonian, we could proceed exactly in the same way. However, at the Newtonian order it is in fact much more efficient to make use of the well-known Fourier decomposition of the Keplerian motion. Using this we can derive the components of the multipole moments (at Newtonian order) as series of combinations of Bessel functions. Then it is a very simple matter to compute numerically the associated "Newtonian" enhancement functions [namely $\varphi(e), \beta(e), \gamma(e)$ and $\chi(e)$]. This is the method which was used in [145]. The relevant expressions of the components of the Newtonian multipole moments, as series of Bessel functions, that we have used to compute numerically the functions $\varphi(e), \beta(e), \gamma(e)$ and $\chi(e)$ are listed in the following subsection.

3.7.1 Fourier coefficients of the multipole moments

In this Section we provide the expressions of the Fourier coefficients of the Newtonian multipole moments in terms of combinations of Bessel functions. Following what we discuss above and [145] we decompose the components of the moments as a Fourier series

$$I_L(t) = \sum_{p=-\infty}^{+\infty} \underset{(p)}{\mathcal{I}_L} e^{ip\ell}, \tag{3.73}$$

$$J_{L-1}(t) = \sum_{p=-\infty}^{+\infty} \underset{(p)}{\mathcal{J}_{L-1}} e^{ip\ell}. \tag{3.74}$$

The Fourier coefficients can been obtained by evaluating the following integrals

$$\underset{(p)}{\mathcal{I}_L} = \frac{1}{2\pi} \int_0^{2\pi} d\ell \, I_L(t) \, e^{-ip\ell}, \tag{3.75}$$

$$\mathop{\mathcal{J}}_{(p)}{}_{L-1} = \frac{1}{2\pi}\int_0^{2\pi} d\ell\, J_{L-1}(t)\, e^{-ip\ell}. \tag{3.76}$$

For the mass quadrupole moment at Newtonian order we have

$$\begin{aligned}
\mathop{\mathcal{I}}_{(p)}{}_{xx} &= \left(\frac{1}{6}+\frac{3}{2}e_t^2\right)J_p(pe_t) \\
&\quad +\left(-\frac{7}{8}e_t-\frac{3}{8}e_t^3\right)\Big(J_{p-1}(pe_t)+J_{p+1}(pe_t)\Big) \\
&\quad +\left(\frac{1}{4}+\frac{1}{4}e_t^2\right)\Big(J_{p-2}(pe_t)+J_{p+2}(pe_t)\Big) \\
&\quad +\left(-\frac{1}{8}e_t+\frac{1}{24}e_t^3\right)\Big(J_{p-3}(pe_t)+J_{p+3}(pe_t)\Big),
\end{aligned} \tag{3.77}$$

$$\begin{aligned}
\mathop{\mathcal{I}}_{(p)}{}_{xy} &= i\sqrt{1-e_t^2}\left\{\frac{5}{8}e_t\Big(-J_{p-1}(pe_t)+J_{p+1}(pe_t)\Big)\right. \\
&\quad +\left(-\frac{1}{4}-\frac{1}{4}e_t^2\right)\Big(J_{p+2}(pe_t)-J_{p-2}(pe_t)\Big) \\
&\quad \left.+\frac{1}{8}e_t\Big(J_{p+3}(pe_t)-J_{p-3}(pe_t)\Big)\right\},
\end{aligned} \tag{3.78}$$

$$\begin{aligned}
\mathop{\mathcal{I}}_{(p)}{}_{yy} &= \left(\frac{1}{6}-e_t^2\right)J_p(pe_t) \\
&\quad +\left(\frac{3}{8}e_t+\frac{1}{4}e_t^3\right)\Big(J_{p-1}(pe_t)+J_{p+1}(pe_t)\Big) \\
&\quad -\frac{\mathrm{I}}{4}\Big(J_{p-2}(pe_t)+J_{p+2}(pe_t)\Big) \\
&\quad +\left(\frac{1}{8}e_t-\frac{1}{12}e_t^3\right)\Big(J_{p-3}(pe_t)+J_{p+3}(pe_t)\Big),
\end{aligned} \tag{3.79}$$

$$\begin{aligned}
\mathop{\mathcal{I}}_{(p)}{}_{zz} &= \left(-\frac{1}{3}-\frac{1}{2}e_t^2\right)J_p(pe_t) \\
&\quad +\left(\frac{1}{2}e_t+\frac{1}{8}e_t^3\right)\Big(J_{p-1}(pe_t)+J_{p+1}(pe_t)\Big) \\
&\quad -\frac{1}{4}e_t^2\Big(J_{p-2}(pe_t)+J_{p+2}(pe_t)\Big) \\
&\quad +\frac{1}{24}e_t^3\Big(J_{p-3}(pe_t)+J_{p+3}(pe_t)\Big).
\end{aligned} \tag{3.80}$$

For the mass octupole moment we find

$$
\begin{aligned}
\underset{(p)}{\mathcal{I}}_{xxx} &= \left(\frac{3}{8}e_t + \frac{11}{8}e_t^3\right)J_p(pe_t) \\
&\quad + \left(-\frac{3}{40} - \frac{21}{20}e_t^2 - \frac{11}{40}e_t^4\right)\Big(J_{p-1}(pe_t) + J_{p+1}(pe_t)\Big) + \\
&\quad \left(\frac{11}{20}e_t + \frac{3}{20}e_t^3\right)\Big(J_{p-2}(pe_t) + J_{p+2}(pe_t)\Big) \\
&\quad + \left(-\frac{1}{8} - \frac{3}{20}e_t^2 + \frac{3}{40}e_t^4\right)\Big(J_{p-3}(pe_t) + J_{p+3}(pe_t)\Big) \\
&\quad + \left(\frac{1}{16}e_t - \frac{3}{80}e_t^3\right)\Big(J_{p-4}(pe_t) + J_{p+4}(pe_t)\Big), \qquad (3.81)
\end{aligned}
$$

$$
\begin{aligned}
\underset{(p)}{\mathcal{I}}_{xxy} &= i\sqrt{1-e_t^2}\left\{\left(\frac{3}{40} + \frac{57}{80}e_t^2\right)\Big(J_{p+1}(pe_t) - J_{p-1}(pe_t)\Big)\right. \\
&\quad + \left(-\frac{11}{20}e_t - \frac{19}{80}e_t^3\right)\Big(J_{p+2}(pe_t) - J_{p-2}(pe_t)\Big) \\
&\quad + \left(\frac{1}{8} + \frac{17}{80}e_t^2\right)\Big(J_{p+3}(pe_t) - J_{p-3}(pe_t)\Big) \\
&\quad \left. + \left(-\frac{1}{16}e_t + \frac{1}{160}e_t^3\right)\Big(J_{p+4}(pe_t) - J_{p-4}(pe_t)\Big)\right\}, \qquad (3.82)
\end{aligned}
$$

$$
\begin{aligned}
\underset{(p)}{\mathcal{I}}_{xyy} &= \left(\frac{3}{8}e_t - \frac{13}{16}e_t^3\right)J_p(pe_t) \\
&\quad + \left(-\frac{3}{40} + \frac{21}{80}e_t^2 + \frac{13}{80}e_t^4\right)\Big(J_{p-1}(pe_t) + J_{p+1}(pe_t)\Big) \\
&\quad + \left(-\frac{13}{40}e_t + \frac{3}{20}e_t^3\right)\Big(J_{p-2}(pe_t) + J_{p+2}(pe_t)\Big) \\
&\quad + \left(\frac{1}{8} + \frac{3}{80}e_t^2 - \frac{9}{80}e_t^4\right)\Big(J_{p-3}(pe_t) + J_{p+3}(pe_t)\Big) \\
&\quad + \left(-\frac{1}{16}e_t + \frac{9}{160}e_t^3\right)\Big(J_{p-4}(pe_t) + J_{p+4}(pet)\Big), \qquad (3.83)
\end{aligned}
$$

$$
\begin{aligned}
\underset{(p)}{\mathcal{I}}_{yyy} &= i\left\{\left(\frac{3}{40} - \frac{3}{5}e_t^2\right)\Big(-J_{p-1}(pe_t) + J_{p+1}(pe_t)\Big)\right. \\
&\quad + \left(\frac{13}{40}e_t + \frac{1}{5}e_t^3\right)\Big(-J_{p-2}(pe_t) + J_{p+2}(pe_t)\Big) \\
&\quad + \left(-\frac{1}{8} - \frac{1}{10}e_t^2\right)\Big(-J_{p-3}(pe_t) + J_{p+3}(pe_t)\Big) \\
&\quad \left. + \left(\frac{1}{16}e_t - \frac{1}{40}e_t^3\right)\Big(-J_{p-4}(pe_t) + J_{p+4}(pe_t)\Big)\right], \qquad (3.84)
\end{aligned}
$$

$$
\underset{(p)}{\mathcal{I}}_{zzx} = \left(-\frac{1}{4}e_t - \frac{3}{16}e_t^3\right)J_p(pe_t)
$$

$$+\left(\frac{1}{20}+\frac{21}{80}e_t^2+\frac{3}{80}e_t^4\right)\Big(J_{p-1}(pe_t)+J_{p+1}(pe_t)\Big)$$
$$+\left(-\frac{3}{40}e_t-\frac{1}{10}e_t^3\right)\Big(J_{p-2}(pe_t)+J_{p+2}(pe_t)\Big)$$
$$+\left(\frac{3}{80}e_t^2+\frac{1}{80}e_t^4\right)\Big(J_{p-3}(pe_t)+J_{p+3}(pe_t)\Big)$$
$$-\frac{1}{160}e_t^3\Big(J_{p-4}(pe_t)+J_{p+4}(pe_t)\Big), \tag{3.85}$$

$$\underset{(p)}{\mathcal{I}_{zzy}} = i\sqrt{1-e_t^2}\left\{\left(-\frac{1}{20}-\frac{3}{80}e_t^2\right)\Big(-J_{p-1}(pe_t)+J_{p+1}(pe_t)\Big)\right.$$
$$+\left(\frac{3}{40}e_t+\frac{1}{80}e_t^3\right)\Big(-J_{p-2}(pe_t)+J_{p+2}(pe_t)\Big)$$
$$-\frac{3}{80}e_t^2\Big(-J_{p-3}(pe_t)+J_{p+3}(pe_t)\Big)$$
$$\left.+\frac{1}{160}e_t^3\Big(-J_{p-4}(pe_t)+J_{p+4}(pe_t)\Big)\right\}. \tag{3.86}$$

Finally, for the current quadrupole moment,

$$\underset{(p)}{\mathcal{J}_{xz}} = \frac{1}{2}\sqrt{1-e_t^2}\left\{3e_tJ_p(pe_t)\right.$$
$$+\left(-1-e_t^2\right)\Big(J_{p-1}(pe_t)+J_{p+1}(pe_t)\Big)$$
$$\left.+\frac{1}{2}e_t\Big(J_{p-2}(pe_t)+J_{p+2}(pe_t)\Big)\right\}, \tag{3.87}$$

$$\underset{(p)}{\mathcal{J}_{yz}} = i\left(1-e_t^2\right)\left\{\Big(J_{p+1}(pe_t)-J_{p-1}(pe_t)\Big)\right.$$
$$\left.-\frac{1}{2}e_t\Big(J_{p+2}(pe_t)-J_{p-2}(pe_t)\Big)\right\}. \tag{3.88}$$

3.8 Final expression of the tail integrals

Based on the treatment outlined above of a numerical scheme for the computation of the orbital average of the hereditary part of the energy flux up to 3PN, we finally provide the complete results for the dimensionless enhancement factors and their numerical plots. It is convenient for the final presentation to redefine in a minor way some of the enhancement functions of Sec. 3.6, which were directly given by simple Fourier decomposition. Let us choose

$$\psi(e) = \frac{13696}{8191}\alpha(e)-\frac{16403}{24573}\beta(e)-\frac{112}{24573}\gamma(e), \tag{3.89}$$

$$\theta'(e) = -\frac{1424}{4081}\theta(e)+\frac{16403}{12243}\beta(e)+\frac{16}{1749}\gamma(e), \tag{3.90}$$

$$\kappa(e) = F(e) + \frac{59920}{116761}\chi(e). \tag{3.91}$$

Considering thus the 1.5PN and 2.5PN terms, composed of tails, and the 3PN terms, composed of tails of tails and tail squared, the total hereditary contribution to the average of the energy flux, normalized to the Newtonian value for circular orbits finally reads

$$\begin{aligned}\mathcal{F}^{\rm 3PN}_{\rm tail} = \frac{32}{5}\nu^2 x^5\Bigg\{4\pi x^{3/2}\varphi(e_t) + \pi x^{5/2}\left[-\frac{8191}{672}\psi(e_t) - \frac{583}{24}\nu\theta'(e_t)\right] \\ + x^3\left[-\frac{116761}{3675}\kappa(e_t) + \left[\frac{16}{3}\pi^2 - \frac{1712}{105}C - \frac{1712}{105}\ln\left(\frac{4\omega r_0}{c}\right)\right]F(e_t)\right]\Bigg\}.\end{aligned} \tag{3.92}$$

All the enhancement functions in Eq. 3.42 are defined in such a way that they reduce to one in the circular case, $e_t = 0$, so that the circular-limit of the formula is immediately seen from inspection of Eq. 3.42, and is seen to be in complete agreement with Refs. [158, 95].

In Eq. 3.42 there are four enhancement functions which probably do not admit any analytic closed-form expressions: these are $\varphi(e_t)$, $\psi(e_t)$, $\theta(e_t)$ and $\kappa(e_t)$. However, $F(e_t)$ is known analytically, and we recall here its expression,

$$F(e_t) = \frac{1 + \frac{85}{6}e_t^2 + \frac{5171}{192}e_t^4 + \frac{1751}{192}e_t^6 + \frac{297}{1024}e_t^8}{(1 - e_t^2)^{13/2}} \tag{3.93}$$

We now present the numerical plots of the four enhancement functions $\varphi(e_t)$, $\psi(e_t)$, $\theta(e_t)$ and $\kappa(e_t)$. We have explained the details of the numerical calculation in Sec. 3.7. The figures display the plots of all these enhancement functions as functions of eccentricity e,.

3.8.1 The Log terms in the total energy flux

As seen from Eq. 3.92 the result depends finally on the constant $r_0 = \tau_0/2$ at the 3PN order. We are now in a position to discuss in detail the structure of the Log term in the complete energy flux, the cancellation of the $\ln r_0$ term and the circular orbit limit of this term for one last final check of this complicated calculation. From Eq. (3.101f), the log terms in the instantaneous contribution to the average flux is given by

$$\frac{32}{5}\nu^2 x^5\left\{\frac{1712}{105}F(e_t)\ln\left[x\left(\frac{c^2 r_0}{Gm}\right)\frac{1 + \sqrt{1 - e_t^2}}{2\left(1 - e_t^2\right)}\right]\right\}. \tag{3.94}$$

Similarly, from Eq. (3.92) the log terms in the tail contribution to the average flux is

$$\frac{32}{5}\nu^2 x^5\left\{-\frac{1712}{105}F(e_t)\ln\left[4x^{3/2}\left(\frac{c^2 r_0}{Gm}\right)\right]\right\}. \tag{3.95}$$

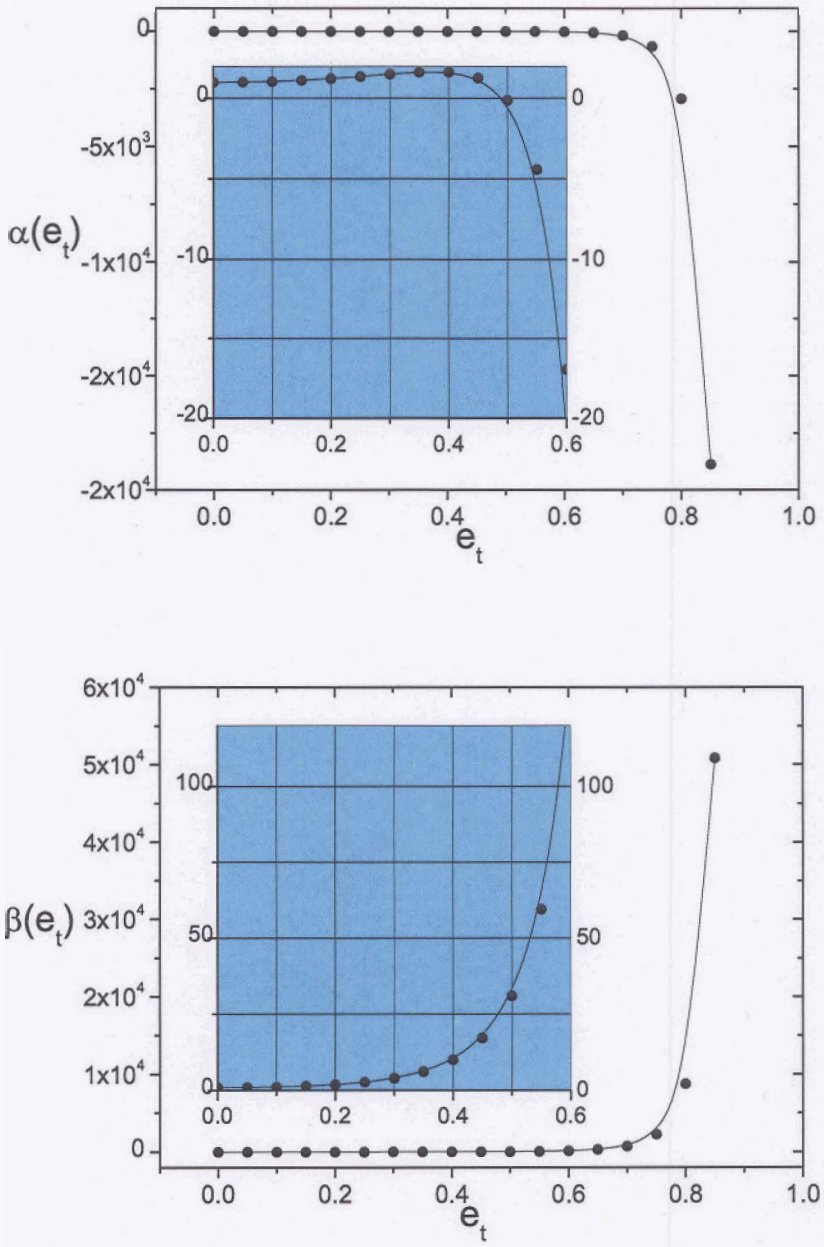

Figure 3.5: This figure shows the variation of $\alpha(e_t)$ and $\beta(e_t)$ with the eccentricity e_t. The plot inside the graph is the zooming for the functions which look as straight horizontal lines in main graph. The dot points **are the numerical** computation **for $\alpha(e_t)$ (top panel)** and $\beta(e_t)$ (bottom **panel) at e_t =0, 0.5, 1, 1.5, ... The solid lines** are **the fitting** for the numerical **points. At the circular** limit, $e_t = 0$, $\alpha(0) = \beta(0) = 1$.

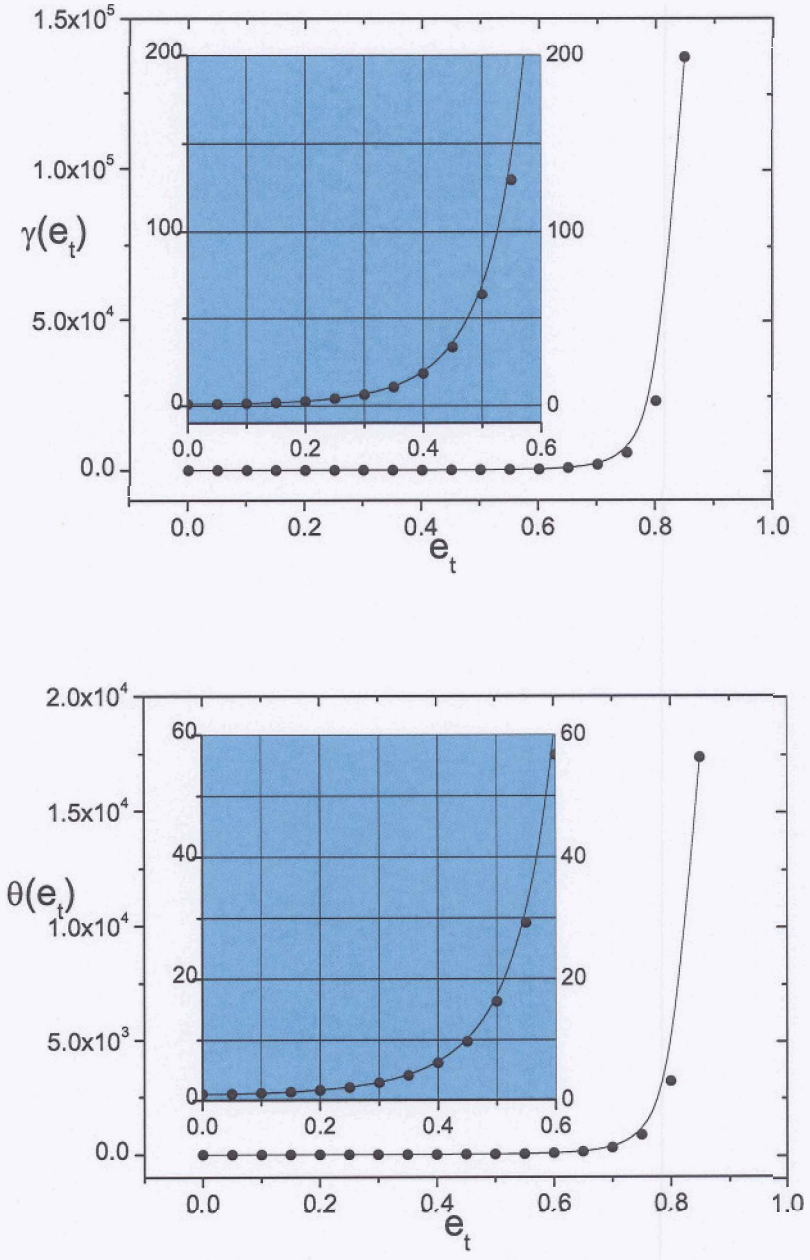

Figure 3.6: **This figure shows the** variation **of** $\gamma(e_t)$ **(top panel) and** $\theta(e_t)$ (bottom panel) **with the eccentricity** e_t. **The plot inside the graph is the zooming for the functions which look as straight horizontal lines in main graph. The dot points are the** numerical **computation for** $\gamma(e_t)$ **and** $\theta(e_t)$ **at** e_t =0, 0.5, 1, 1.5, ... The **solid lines are the fitting for the numerical, points. At the circular** limit, $e_t = 0$, $\gamma(0) = \theta(0) = 1$.

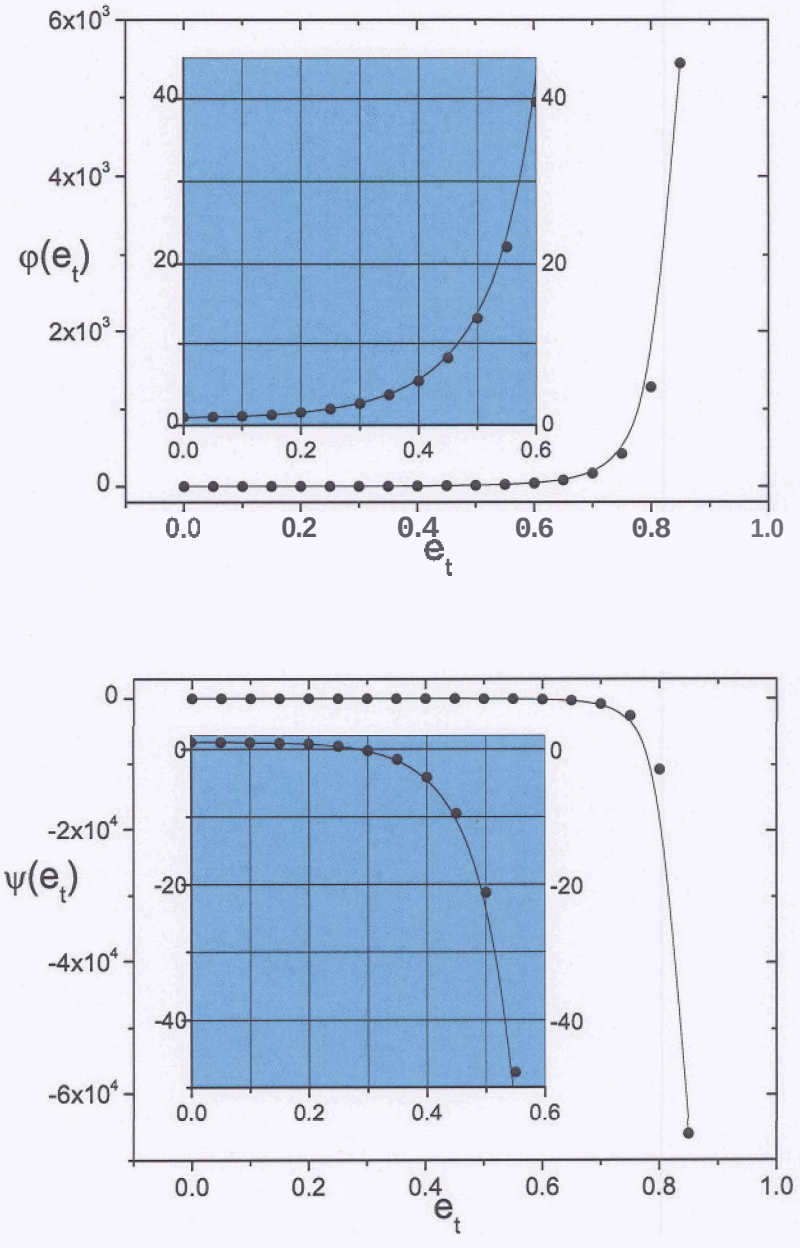

Figure 3.7: This figure shows the variation of $\phi(e_t)$ (top panel) and $\psi(e_t)$ **(bottom panel) with the** eccentricity e_t. **The plot inside the graph is** the zooming for **the** functions which **look as** straight horizontal **lines** in main **graph. The** dot **points are the** numerical **computation** for $\phi(e_t)$ **and** $\psi(e_t)$ **at** e_t =0, 0.5, 1, 1.5,.... The **solid lines are the fitting for the** numerical **points. At** the **circular** limit, $e_t = 0$, $\phi(0) = \psi(0) = 1$.

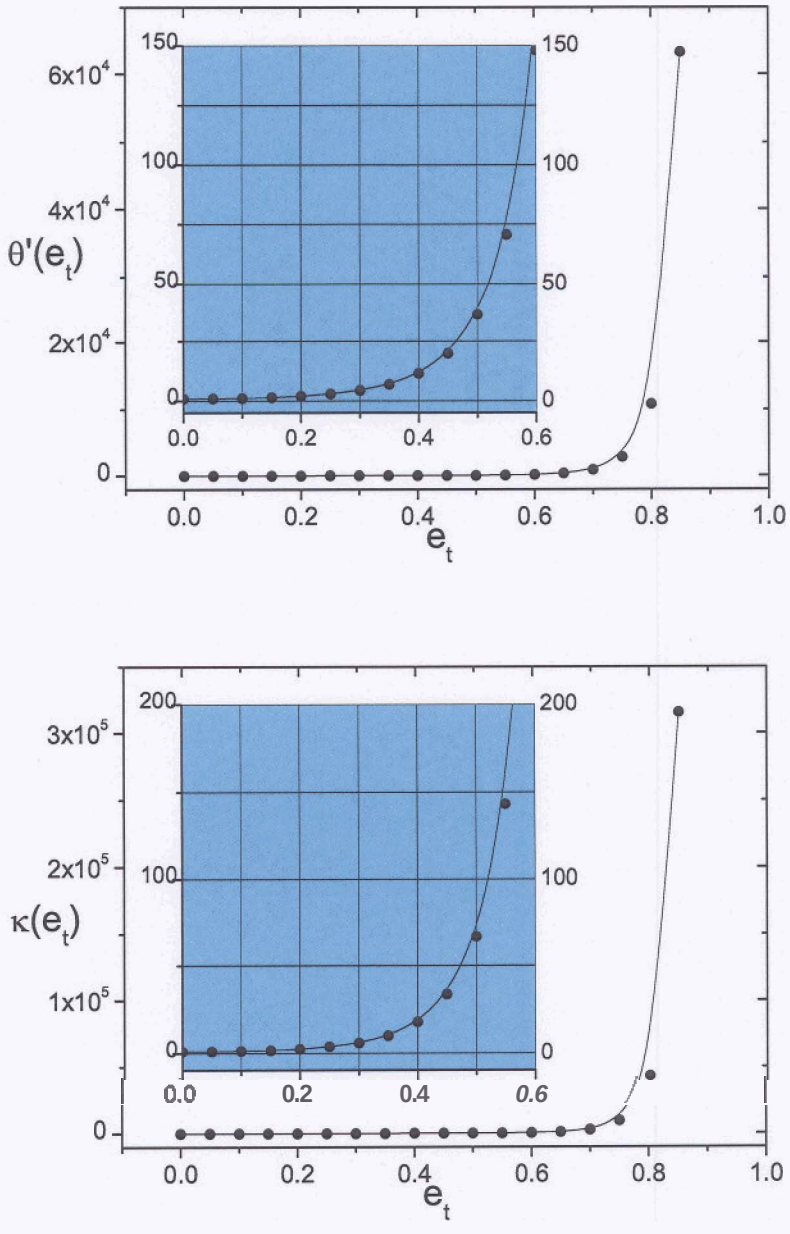

Figure 3.8: This figure shows the variation of $\theta'(e_t)$ (top panel) and $\kappa(e_t)$ (bottom panel) with the eccentricity e_t. The plot inside the graph is the zooming for the functions which look as straight horizontal lines in main graph. The dot points are the numerical computation for $\theta'(e_t)$ and $\kappa(e_t)$ at e_t =0, 0.5, 1, 1.5,.... The solid lines are the fitting for the numerical points. At the circular limit, $e_t = 0$, $\theta'(0) = \kappa(0) = 1$.

Table 3.1: The table listed the numerical variation of all enhancement functions with eccentricity e_t

e_t	$\alpha(e_t)$	$\beta(e_t)$	$\gamma(e_t)$	$\theta(e_t)$	$\phi(e_t)$	$\theta'(e_t)$	$\psi(e_t)$	$F(e_t)$	$\chi(e_t)$	$\kappa(e_t)$
0	1.000	1.000	1.000	1.000	1.000	1.000	1.000	1.000	0	1.000
0.05	1.015	1.047	1.076	1.032	1.031	1.052	0.9925	1.053	0.02673	1.066
0.1	1.058	1.197	1.324	1.133	1.127	1.221	0.9646	1.222	0.1172	1.282
0.15	1.133	1.481	1.803	1.319	1.304	1.540	0.8971	1.545	0.3071	1.702
0.2	1.237	1.959	2.637	1.623	1.588	2.082	0.7492	2.100	0.6738	2.445
0.25	1.370	2.745	4.059	2.104	2.027	2.981	0.4401	3.032	1.376	3.737
0.3	1.519	4.045	6.510	2.865	2.702	4.480	–0.1907	4.615	2.738	6.020
0.35	1.647	6.251	10.84	4.094	3.757	7.045	−1.468	7.380	5.451	10.18
0.4	1.656	10.12	18.75	6.146	5.447	11.59	–4.073	12.40	11.04	18.07
0.45	1.290	17.23	33.85	9.724	8.254	20.00	–9.499	21.98	23.08	33.82
0.5	–0.1238	31.00	64.19	16.31	13.13	36.44	−21.20	41.32	50.43	67.20
0.55	–4.423	59.49	129.2	29.23	22.07	70.69	–47.70	83.24	116.9	143.2
0.6	−16.94	123.4	279.7	56.76	39.63	148.0	−112.0	182.3	292.6	332.4
0.65	−54.65	281.8	664.6	121.7	77.23	341.2	−282.5	443.1	810.1	858.8
0.7	−178.7	729.5	1785.	296.2	167.3	890.4	−794.0	1233.	2567.	2551.
0.75	−652.1	2239.	5665.	856.3	417.9	2753.	−2611.	4127.	9805.	9159.
0.8	−2928.	8789.	2.294×10^4	3172.	1282.	1.088×10^4	-1.087×10^4	1.802×10^4	4.921×10^4	4.328×10^4
0.85	-1.887×10^4	5.084×10^4	1.366×10^5	1.734×10^4	5440.	6.332×10^4	-6.612×10^4	1.198×10^5	3.811×10^5	3.153×10^5
0.9	-2.421×10^5	5.960×10^5	1.647×10^6	1.926×10^5	4.163×10^4	7.464×10^5	-8.102×10^5	1.712×10^6	6.519×10^6	5.058×10^6

Summing up, we have for the ***log terms in the total 3PN energy flux***

$$-\frac{32\nu^2 x^5}{5}\frac{1712}{105}F(e_t)\ln\left[\frac{8\sqrt{x}\left(1-e_t^2\right)}{1+\sqrt{1-e_t^2}}\right]. \tag{3.96}$$

The dependence on r_0 cancels as expected from general considerations providing a check on our algebra. Moreover, in the circular limit, $F(0) = 1$ and the net result for the log term in the average flux is $-\frac{856}{105}\ln 16\,x$, in perfect agreement with [95].

After the above explicit check of our computation, let us understand in bit more detail the occurence of this constant. We first remind from [158] that the dependence of the radiative-type quadrupole moment at infinity, say U_{ij}, in terms of the constant r_0 arises at 3PN order, exclusively from the tails of tails (*i.e.* the multipole interaction $\propto M^2 \times I_{ij}$), and is explicitly given by

$$U_{ij}(t) = I_{ij}^{(3)}(\mathrm{t}) + \ldots + \frac{214}{105}M^2 I_{ij}^{(4)}(\mathrm{t})\ln r_0 + \ldots, \tag{3.97}$$

where we indicate that at the lowest Newtonian order U_{ij} reduces to the second time derivative of I_{ij}, and where the dots indicate all the terms which do not depend on r_0. From this it is then trivial to deduce that the corresponding dependence of the tail part of the energy flux on r_0 is given by

$$\mathcal{F}_{\mathrm{tail}} = \cdots - \frac{428}{525}M^2\langle I_{ij}^{(4)}I_{ij}^{(4)}\rangle \ln r_0 + \cdots, \tag{3.98}$$

where we have taken advantage of the fact that inside the time average operation $\langle\rangle$ one can freely operate by parts the time derivatives. Hence, we wrote $\langle I_{ij}^{(3)}I_{ij}^{(5)}\rangle = -\langle I_{ij}^{(4)}I_{ij}^{(4)}\rangle$ to arrive at the result 3.98. Thus, the effect 3.98 looks like a "quadrupole formula" but where the third time derivative of the moment is replaced by the fourth one. Notice that the far zone total energy flux in Eq. (2.1) is true for any post-Newtonian source, and in particular for a binary system moving on eccentric orbit. From this one readily infers that the dependence on eccentricity e_t of the coefficient of $\ln r_0$ in Eq. 3.89 must necessarily be given by the function

$$F(e_t) = \frac{\omega^8}{128}\langle\hat{I}_{ij}^{(4)}\hat{I}_{ij}^{(4)}\rangle = \frac{1}{64}\sum_{p=1}^{+\infty}p^8|\hat{I}_{ij}|^2, \tag{3.99}$$

in which we made use of the reduced quadrupole moment defined by Eq. 3.52a. The result is thus perfectly in agreement with our finding of the function $F(e)$ in Eq. 3.62. The dependence of the tail part of the averaged energy flux on the constant r_0 is such that it cancels out, for any value of the eccentricity, with a similar term coming from the instantaneous part of the flux. Of course such cancellation must be true for any source, and can be shown based on general arguments in [158], but for the present case it gives an interesting check of our calculations.

3.9 The complete 3PN energy flux

At long last, we are now in a position to write down the ***complete* 3PN** GW energy flux averaged over an orbit for an ICB moving in an elliptical orbit. Summing up the averaged instantaneous contribution of Eq. **3.100** and the tail contribution Eq. **3.92** the orbital average of the energy flux in the modified harmonic coordinates is:

$$\begin{aligned} <\dot{\mathcal{E}}>_{\rm MHar} &= \frac{32\nu^2 x^5}{5}\frac{1}{\left(1-e_t^2\right)^{7/2}}\Big(<\dot{\mathcal{E}}_N>_{\rm MHar} + x <\dot{\mathcal{E}}_{1PN}>_{\rm MHar} \\ &\quad + x^{3/2} <\dot{\mathcal{E}}_{3/2PN}>_{\rm MHar} + x^2 <\dot{\mathcal{E}}_{2PN}>_{\rm MHar} \\ &\quad + x^{5/2} <\dot{\mathcal{E}}_{5/2PN}>_{\rm MHar} + x^3 <\dot{\mathcal{E}}_{3PN}>_{\rm MHar}\Big) . \end{aligned} \tag{3.100}$$

$$<\dot{\mathcal{E}}_N>_{\rm Mhar} = 1 + e_t^2\frac{73}{24} + e_t^4\frac{37}{96}, \tag{3.101a}$$

$$\begin{aligned} <\dot{\mathcal{E}}_{\rm 1PN}>_{\rm Mhar} &= \frac{1}{\left(1-e_t^2\right)} \\ &\quad \left\{\left(-\frac{1247}{336}-\frac{35}{12}\nu\right) + e_t^2\left(\frac{10475}{672}-\frac{1081}{36}\nu\right)\right. \\ &\quad \left. + e_t^4\left(\frac{10043}{384}-\frac{311}{12}\nu\right) + e_t^6\left(\frac{2179}{1792}-\frac{851}{576}\nu\right)\right\}, \end{aligned} \tag{3.101b}$$

$$<\dot{\mathcal{E}}_{\rm 1.5PN}>_{\rm Mhar} = 4\pi\,\varphi(e_t), \tag{3.101c}$$

$$\begin{aligned} <\dot{\mathcal{E}}_{\rm 2PN}>_{\rm Mhar} &= \frac{1}{\left(1-e_t^2\right)^2} \\ &\quad \left\{-\frac{203471}{9072}+\frac{12799}{504}\nu+\frac{65}{18}\nu^2 + e_t^2\left(-\frac{3807197}{18144}+\frac{116789}{2016}\nu+\frac{5935}{54}\nu^2\right)\right. \\ &\quad + e_t^4\left(-\frac{268447}{24192}-\frac{2465027}{8064}\nu+\frac{247805}{864}\nu^2\right) \\ &\quad + e_t^6\left(\frac{1307105}{16128}-\frac{416945}{2688}\nu+\frac{185305}{1728}\nu^2\right) \\ &\quad + e_t^8\left(\frac{86567}{64512}-\frac{9769}{4608}\nu+\frac{21275}{6912}\nu^2\right) \\ &\quad + \sqrt{1-e_t^2}\left[\left(\frac{35}{2}-7\nu\right) + e_t^2\left(\frac{6425}{48}-\frac{1285}{24}\nu\right)\right. \\ &\quad \left.\left. + e_t^4\left(\frac{5065}{64}-\frac{1013}{32}\nu\right) + e_t^6\left(\frac{185}{96}-\frac{37}{48}\nu\right)\right]\right\}, \end{aligned} \tag{3.101d}$$

$$<\dot{\mathcal{E}}_{\rm 2.5PN}>_{\rm Mhar} = \pi\left[-\frac{8191}{672}\psi(e_t) - \frac{583}{24}\nu\,\theta'(e_t)\right], \tag{3.101e}$$

$$
\begin{aligned}
< \dot{\mathcal{E}}_{3\mathrm{PN}} >_{\mathrm{Mhar}} \;=\; & \frac{1}{\left(1-e_t^2\right)^3} \\
& \left\{ \frac{1266161801}{9979200} + \left(\frac{8009293}{54432} - \frac{41}{64}\pi^2 \right)\nu - \frac{94403}{3024}\nu^2 - \frac{775}{324}\nu^3 \right. \\
& + e_t^2 \left(\frac{27805251167}{19958400} + \left[\frac{654126203}{272160} + \frac{4879}{1536}\pi^2 \right]\nu - \frac{1179281}{3024}\nu^2 - \frac{53696}{243}\nu^3 \right) \\
& + e_t^4 \left(\frac{670405291}{415800} + \left[\frac{763187017}{136080} - \frac{29971}{1024}\pi^2 \right]\nu + \frac{142865}{192}\nu^2 - \frac{10816087}{7776}\nu^3 \right) \\
& + e_t^6 \left(\frac{1121282527}{1478400} + \left[\frac{1147175951}{1451520} - \frac{84501}{4096}\pi^2 \right]\nu + \frac{100111945}{48384}\nu^2 - \frac{983251}{648}\nu^3 \right) \\
& + e_t^8 \left(\frac{22052148101}{141926400} + \left[-\frac{32334863}{129024} - \frac{4059}{4096}\pi^2 \right]\nu + \frac{80211601}{193536}\nu^2 - \frac{4586539}{15552}\nu^3 \right) \\
& + e_t^{10} \left(-\frac{8977637}{11354112} + \frac{9287}{48384}\nu + \frac{8977}{55296}\nu^2 - \frac{567617}{124416}\nu^3 \right) \\
& + \sqrt{1-e_t^2} \left[\left(-\frac{165761}{1008} + \frac{287}{192}\pi^2 \right)\nu + e_t^2 \left(-\frac{14935421}{6048} + \frac{52685}{4608}\pi^2 \right)\nu \right. \\
& + e_t^4 \left(-\frac{31082483}{8064} + \frac{41533}{6144}\pi^2 \right)\nu + e_t^6 \left(-\frac{40922933}{48384} + \frac{1517}{9216}\pi^2 \right)\nu \\
& \left. + e_t^8 \left(-\frac{1073}{288}\nu \right) \right] + (1-e_t^2)^{13/2} \left[\left(\frac{16}{3}\pi^2 - \frac{1712}{105} \ln \left[\frac{8\sqrt{x}\left(1-e_t^2\right)}{1+\sqrt{1-e_t^2}} \right] \right. \right. \\
& \left. \left. - \frac{1712}{105} C \right) F(e_t) - \frac{116761}{3675} \kappa(e_t) \right] \Bigg\} . \qquad (3.101\mathrm{f})
\end{aligned}
$$

Recall that the e_t above denotes e_t^{Mhar}. Similarly, the total orbital average of the energy **flux** in the ADM coordinates is given by:

$$
\begin{aligned}
< \dot{\mathcal{E}} >_{\mathrm{ADM}} \;=\; & \frac{32\nu^2 x^5}{5} \frac{1}{\left(1-e_t^2\right)^{7/2}} \left(< \dot{\mathcal{E}}_N >_{\mathrm{ADM}} + x < \dot{\mathcal{E}}_{1PN} >_{\mathrm{ADM}} \right. \\
& + x^{3/2} < \dot{\mathcal{E}}_{3/2PN} >_{\mathrm{ADM}} + x^2 < \dot{\mathcal{E}}_{2PN} >_{\mathrm{ADM}} \\
& \left. + x^{5/2} < \dot{\mathcal{E}}_{5/2PN} >_{\mathrm{ADM}} + x^3 < \dot{\mathcal{E}}_{3PN} >_{\mathrm{ADM}} \right) . \qquad (3.102)
\end{aligned}
$$

$$
< \dot{\mathcal{E}}_N >_{\mathrm{ADM}} \;=\; 1 + e_t^2 \frac{73}{24} + e_t^4 \frac{37}{96} , \qquad (3.103\mathrm{a})
$$

$$
\begin{aligned}
< \dot{\mathcal{E}}_{1\mathrm{PN}} >_{\mathrm{ADM}} \;=\; & \frac{1}{\left(1-e_t^2\right)} \left\{ \left(\left(-\frac{1247}{336} - \frac{35}{12}\nu \right) + e_t^2 \left(\frac{10475}{672} - \frac{1081}{36}\nu \right) \right. \right. \\
& \left. \left. + e_t^4 \left(\frac{10043}{384} - \frac{311}{12}\nu \right) + e_t^6 \left(\frac{2179}{1792} - \frac{851}{576}\nu \right) \right) \right\} , \qquad (3.103\mathrm{b})
\end{aligned}
$$

$$< \dot{\mathcal{E}}_{1.5\mathrm{PN}} >_{\mathrm{ADM}} = 4\pi\,\varphi(e_t)\,, \tag{3.103c}$$

$$\begin{aligned} < \dot{\mathcal{E}}_{2\mathrm{PN}} >_{\mathrm{ADM}} = {} & \frac{1}{\left(1-e_t^2\right)^2} \\ & \left\{-\frac{203471}{9072}+\frac{12799}{504}\nu+\frac{65}{18}\nu^2+e_t^2\left(-\frac{3866543}{18144}+\frac{4691}{2016}\nu+\frac{5935}{54}\nu^2\right)\right. \\ & +e_t^4\left(-\frac{369751}{24192}-\frac{3039083}{8064}\nu+\frac{247805}{864}\nu^2\right) \\ & +e_t^6\left(\frac{1302443}{16128}-\frac{215077}{1344}\nu+\frac{185305}{1728}\nu^2\right) \\ & +e_t^8\left(\frac{86567}{64512}-\frac{9769}{4608}\nu+\frac{21275}{6912}\nu^2\right) \\ & +\sqrt{1-e_t^2}\left[\frac{35}{2}-7\nu+e_t^2\left(\frac{6425}{48}-\frac{1285}{24}\nu\right)\right. \\ & \left.\left.+e_t^4\left(\frac{5065}{64}-\frac{1013}{32}\nu\right)+e_t^6\left(\frac{185}{96}-\frac{37}{48}\nu\right)\right]\right\}, \end{aligned} \tag{3.103d}$$

$$< \dot{\mathcal{E}}_{2.5\mathrm{PN}} >_{\mathrm{ADM}} = \pi\left[-\frac{8191}{672}\,\psi(e_t)-\frac{583}{24}\nu\,\theta'(e_t)\right], \tag{3.103e}$$

$$\begin{aligned} < \dot{\mathcal{E}}_{3\mathrm{PN}} >_{\mathrm{ADM}} = {} & \frac{1}{\left(1-e_t^2\right)^3} \\ & \left\{\frac{1266161801}{9979200}+\left[\frac{8009293}{54432}-\frac{41}{64}\pi^2\right]\nu-\frac{94403}{3024}\nu^2-\frac{775}{324}\nu^3\right. \\ & +e_t^2\left(\frac{27685797767}{19958400}+\left[\frac{250838045}{108864}+\frac{31255}{1536}\pi^2\right]\nu+\frac{133487}{6048}\nu^2-\frac{53696}{243}\nu^3\right) \\ & +e_t^4\left(\frac{5135886353}{3326400}+\left[\frac{479870915}{108864}-\frac{7459}{1024}\pi^2\right]\nu+\frac{1305967}{576}\nu^2-\frac{10816087}{7776}\nu^3\right) \\ & +e_t^6\left(\frac{352339259}{492800}+\left[-\frac{4938799}{145152}-\frac{78285}{4096}\pi^2\right]\nu+\frac{34228207}{12096}\nu^2-\frac{983251}{648}\nu^3\right) \\ & +e_t^8\left(\frac{21840664301}{141926400}+\left[-\frac{36513893}{129024}-\frac{4059}{4096}\pi^2\right]\nu+\frac{86104369}{193536}\nu^2-\frac{4586539}{15552}\nu^3\right) \\ & +e_t^{10}\left(-\frac{8977637}{11354112}+\frac{9287}{48384}\nu+\frac{8977}{55296}\nu^2-\frac{567617}{124416}\nu^3\right) \\ & +\sqrt{1-e_t^2}\left[\left(-\frac{165761}{1008}+\frac{287}{192}\pi^2\right)\nu+e_t^2\left(-\frac{14935421}{6048}+\frac{52685}{4608}\pi^2\right)\nu\right. \\ & +e_t^4\left(-\frac{31082483}{8064}+\frac{41533}{6144}\pi^2\right)\nu+e_t^6\left(-\frac{40922933}{48384}+\frac{1517}{9216}\pi^2\right)\nu \\ & \left.+e_t^8\left(-\frac{1073}{288}\nu\right)\right]+(1-e_t^2)^{13/2}\left[\left(\frac{16}{3}\pi^2-\frac{1712}{105}\ln\left[\frac{8\sqrt{x}\left(1-e_t^2\right)}{1+\sqrt{1-e_t^2}}\right]\right.\right. \\ & \left.\left.\left.-\frac{1712}{105}C\right)F(e_t)-\frac{116761}{3675}\kappa(e_t)\right]\right\}. \end{aligned} \tag{3.103f}$$

Beware that the e_t above denotes $e_t^{\rm ADM}$.

The circular orbit limit of the above expressions is obtained by setting $e_t = 0$ and

$$F(e_t = 0) = \phi(e_t = 0) = \psi'(e_t = 0) = \theta'(e_t = 0) = \kappa(e_t = 0) = 1\,. \tag{3.104}$$

As expected both from Eqs. 3.100 and 3.102 one obtains,

$$\begin{aligned} <\dot{\mathcal{E}}>|_{\odot} \;=\; & \frac{32}{5}x^5\nu^2\Bigg\{1 + x\left(-\frac{1247}{336} - \frac{35}{12}\nu\right) + 4\pi x^{3/2} \\ & + x^2\left(-\frac{44711}{9072} + \frac{9271}{504}\nu + \frac{65}{18}\nu^2\right) - \pi x^{5/2}\left(\frac{8191}{672} + \frac{583}{24}\nu\right) \\ & + x^3\left(\frac{6643739519}{69854400} + \frac{16}{3}\pi^2 - \frac{1712}{105}C - \frac{856}{105}\ln(16x)\right. \\ & \left. + \left[-\frac{14930989}{272160} + \frac{41}{48}\pi^2 - \frac{88}{3}\theta\right]\nu - \frac{94403}{3024}\nu^2 - \frac{775}{324}\nu^3\right)\Bigg\} \end{aligned} \tag{3.105}$$

The above expression is in exact agreement with Eq. (12.9) of [95].

3.10 The test particle limit of the 3PN energy flux

In the previous chapter we obtained the contribution of the ***instantaneous*** terms in the energy flux in the test particle limit to order e_t^2. It is given by:

$$\begin{aligned} \dot{\mathcal{E}}^{\rm Inst.}_{\nu\to 0} \;=\; & \frac{32}{5}\nu^2 x^5 \\ & \Bigg\{1 - \frac{1247}{336}x - \frac{44711}{9072}x^2 + x^3\left(\frac{1266161801}{9979200} + \frac{1712}{105}\ln\left[\frac{c^2 r_0}{Gm}x\right]\right) + \\ & e_t^2\left(\frac{157}{24} - \frac{187}{168}x - \frac{84547}{756}x^2 + x^3\left(\frac{22718275589}{9979200} + \frac{1712}{105}\ln\left[\frac{c^2 r_0}{Gm}x\right]\right)\right)\Bigg\} \\ & + O(e_t^4). \end{aligned} \tag{3.106}$$

In what follows we shall consider the test particle limit of the ***tail*** contributions in our computation. From Eq. 3.92 it is given by:

$$\begin{aligned} \dot{\mathcal{E}}^{\rm Tail}_{\nu\to 0} \;=\; & \frac{32}{5}\nu^2 x^5\Bigg\{4\pi x^{3/2}\varphi(e_t) - \frac{8191}{672}\pi x^{5/2}\psi(e_t) \\ & + x^3\left[-\frac{116761}{3675}\left(F(e_t) + \frac{59920}{116761}\chi(e_t)\right) + \right. \\ & \left.\left(\frac{16}{3}\pi^2 - \frac{1712}{105}C - \frac{1712}{105}\ln\left[4\frac{c^2 r_0}{Gm}x^{3/2}\right]\right)F(e_t)\right]\Bigg\} \\ & + O(e_t^4)\,. \end{aligned} \tag{3.107}$$

To proceed further, the enhancement function should be expanded up to power e_t^2. Let us assume that they are expanded as:

$$F(e_t) = 1 + a_F e_t^2 + O\left(e_t^4\right), \tag{3.108a}$$

$$\varphi(e_t) = 1 + a_\varphi e_t^2 + O\left(e_t^4\right), \tag{3.108b}$$

$$\psi(e_t) = 1 + a_\psi e_t^2 + O(e_t^4), \tag{3.108c}$$

$$\chi(e_t) = a_\chi e_t^2 + O(e_t^4), \tag{3.108d}$$

where a_F, $a_,$, a_ψ and a_χ are pure numbers.
After substituting Eqs. (3.108a)-(3.108d) the tail part in the test particle limit becomes:

$$\begin{aligned}\dot{\mathcal{E}}^{\text{Tail}}_{\nu\to 0} = \frac{32}{5}\nu^2 x^5 \Bigg\{ & 4\pi x^{3/2} - \frac{8191}{672}\pi x^{5/2} + x^3\left(-\frac{116761}{3675} - \frac{1712C}{105} + \frac{16\pi^2}{3}\right. \\ & \left. -\frac{1712}{105}\ln\left[4\frac{c^2 r_0}{Gm}x^{3/2}\right]\right) \\ & + e_t^2\Bigg[4\pi a_\varphi x^{3/2} + -\frac{8191}{672}\pi a_\psi x^{5/2} + x^3\Bigg\{-\frac{1712}{105}a_\chi \\ & + a_F\left(-\frac{116761}{3675} - \frac{1712C}{105} + \frac{16\pi^2}{3} - \frac{1712}{105}\ln\left[4\frac{c^2 r_0}{Gm}x^{3/2}\right]\right)\Bigg\}\Bigg]\Bigg\} + O(e_t^4)\end{aligned} \tag{3.109}$$

Summing up the instantaneous and tail parts then gives the following result for the complete 3PN energy flux in the test particle limit. We have,

$$\begin{aligned}\dot{\mathcal{E}}^{\text{MPM}}_{\nu\to 0} = \frac{32}{5}\nu^2 x^5 \Bigg\{ & 1 - \frac{1247}{336}x + 4\pi x^{3/2} - \frac{44711x^2}{9072} - \frac{8191}{672}\pi x^{5/2} \\ & + x^3\left(\frac{6643739519}{69854400} - \frac{1712C}{105} + \frac{16\pi^2}{3} - \frac{3424}{105}\ln[2] - \frac{856}{105}\ln[x]\right) \\ & + e_t^2\Bigg[\frac{157}{24} - \frac{187x}{168} + 4a_\phi\pi x^{3/2} - \frac{84547}{756}x^2 - \frac{8191}{672}a_\psi\pi x^{5/2} \\ & + x^3\Bigg(\frac{22718275589}{9979200} - \left(\frac{116761}{3675} + \frac{1712C}{105}\right)a_F - \frac{1712}{105}a_\chi \\ & + \left(-\frac{106144}{315} + \frac{1712}{105}a_F\right)\ln\left[\frac{Gm}{r_0}\right] + \left(\frac{16\pi^2}{3} - \frac{3424}{105}\ln[2]\right)a_F \\ & + \left(\frac{106144}{315} - \frac{856}{35}a_F\right)\ln(x)\Bigg)\Bigg]\Bigg\},\end{aligned} \tag{3.110}$$

The above expression is in terms of our chosen eccentricity e_t. One should beware that the eccentricity appearing in [162] could in general be different and hence the MPM and perturbation results can only compared modulo a transformation of these eccentricities. Lets

assume that the two eccentricities are connected by:

$$e_t^2 = e^2\left(e_0 + e_1\, x + e_2\, x^2 + e_3\, x^3\right). \tag{3.111}$$

In terms of the new Schwarzschild eccentricity the total energy flux thus becomes:

$$\begin{aligned}
\dot{\mathcal{E}}_{\nu\to 0}^{(\mathrm{MPM})} \;=\; & \left\{1 - \frac{1247}{336}x + 4\pi x^{3/2} - \frac{44711}{9072}x^2 - \frac{8191}{672}\pi x^{5/2} + \right. \\
& x^3\left(\frac{6643739519}{69854400} - \frac{1712C}{105} + \frac{16\pi^2}{3} - \frac{3424}{105}\ln[2] - \frac{856}{105}\ln[x]\right) \\
& + e^2\left[\frac{157}{24}e_0 + \left(-\frac{187}{168}e_0 + \frac{157}{24}e_1\right)x + 4\pi x^{3/2} a_\phi\, e_0\right. \\
& + \left(-\frac{84547}{756}\,e_0 - \frac{187}{168}\,e_1 + \frac{157}{24}\,e_2\right)x^2 \\
& + x^{5/2}\left(4\pi a_\phi\, e_1 - \frac{8191}{672}\pi a_\psi\, e_0\right) \\
& + x^3\left\{-\frac{84547}{756}\,e_1 - \frac{187}{168}\,e_2 + \frac{157}{24}\,e_3\right. \\
& + \left(\frac{22718275589}{9979200} - \frac{1712}{105}a_\chi\right)e_0 \\
& + \left(-\frac{116761}{3675} - \frac{1712C}{105} + \frac{16\pi^2}{3}\right)a_F\, e_0 \\
& - \frac{3424}{105}\ln(2)\, a_F\, e_0 + \ln(x)\left(\frac{106144}{315} - \frac{856}{35}\,a_F\right)e_0 \\
& \left.\left. + \ln\left(\frac{Gm}{r_0}\right)\left(-\frac{106144}{315} + \frac{1712}{105}a_F\right)e_0\right]\right\}\Big\} + O(e_t^4).
\end{aligned} \tag{3.112}$$

On the other hand, from the perturbation treatment of Sasaki and Tagoshi [162], the energy flux (in our notation) is given by:

$$\begin{aligned}
\dot{\mathcal{E}}_{\nu\to 0}^{(\mathrm{ST})} \;=\; & \frac{32}{5}\nu^2 x^5 \\
& \left\{1 - \frac{1247}{336}\,x + 4\,\pi x^{3/2} - \frac{44711}{9072}\,x^2 - \frac{8191}{672}\,\pi x^{5/2} + \right. \\
& x^3\left(\frac{6643739519}{69854400} - \frac{1712C}{105} + \frac{16\pi^2}{3} - \frac{3424}{105}\ln[2] - \frac{856}{105}\ln[x]\right) \\
& + e^2\left[\frac{157}{24} - \frac{6781}{168}x + \frac{2335}{48}\,\pi x^{3/2} - \frac{14929\,x^2}{189} - \frac{773}{3}\,\pi x^{5/2} + \right. \\
& x^3\left(\frac{156066596771}{69854400} - \frac{106144C}{315} + \frac{992\pi^2}{9} - \frac{80464\ln[2]}{315} - \frac{234009\ln[3]}{560} - \right. \\
& \left.\left.\left.\frac{5372}{315}\ln[x]\right)\right]\right\} + O(e_t^4)
\end{aligned} \tag{3.113}$$

A direct comparison between the MPM result Eq. 3.112 and the black hole perturbation result Eq. 3.113 then yields:

- Terms independent of e *i.e* the circular orbit contributions are in full agreement.
- The e^2 term: Comparing the coefficients at N, 1PN, 2PN and 3PN yields $e_0 = 1$, $e_1 = -6$, $e_2 = 4$, and finally $a_F = \frac{62}{3}$ respectively. The value of a_F obtained from $x^3 \ln x$ is consistent with the fact that the coefficient of $x^3 \ln(Gm/r_0)$ must be zero, as also from an expansion of the function $F(e_t)$.
- Substituting the above values and comparing the two results, one finally finds:
- $a_\varphi = \frac{2335}{192}$, $a_\psi = -\frac{22988}{8191}$, $a_\chi = -\frac{77}{3}\ln[2] + \frac{6561}{256}\ln[3]$ and $e_3 = -8$.
- To summarise:

$$F(e_t) = 1 + \frac{62}{3}e_t^2 + O\left(e_t^4\right), \tag{3.114a}$$

$$e_t^2 \rightarrow e^2\left(1 - 6x + 4x^2 - 8x^3\right), \tag{3.114b}$$

$$\varphi(e_t) = 1 + \frac{2335}{192}e_t^2 + O\left(e_t^4\right), \tag{3.114c}$$

$$\psi(e_t) = 1 - \frac{22988}{8191}e_t^2 + O\left(e_t^4\right), \tag{3.114d}$$

$$\chi(e_t) = \left(-\frac{77}{3}\ln[2] + \frac{6561}{256}\ln[3]\right)e_t^2 + O\left(e_t^4\right). \tag{3.114e}$$

Using the above expressions in the test particle limit, let's calculate the relative error between the numerical values and the values of the enhancement functions found by comparing the energy flux results above. We find,

1. $F(e_t)$
   at $e_t = 0.001$ the relative error is $1.43 \times 10^{-8}\%$.
   at $e_t = 0.01$ the relative error is 0.000143154%.
   at $e_t = 0.1$ the relative error is 1.22433%.
2. $\varphi(e_t)$
   at $e_t = 0.001$ the relative error is $3.416 \times 10^{-7}\%$.
   at $e_t = 0.01$ the relative error is $2.117 \times 10^{-5}\%$.
   at $e_t = 0.1$ the relative error is 0.508%.
3. $\psi(e_t)$
   at $e_t = 0.05$ the relative error is 0.044%.
   at $e_t = 0.1$ the relative error is 0.761%.

4. $\chi(e_t)$

   at e, = 0.005 the relative error is 0.0425%.

   at e_t = 0.01 the relative error is 0.1351%.

   at e, = 0.05 the relative error is 3.0496%.

   at e, = 0.1 the relative error is 11.5796%.

Note that we take small values for e,, because the expansion is up to e^2 only.

3.10.1 Analytical comparison

The comparison with the perturbation results can also be attempted analytically by implementing from the start the calculation of the tails in the test particle limit and to order e_t^2. For the function F which is given by:

$$F(e) = \frac{1}{64}\sum_{p=1}^{+\infty} p^8 |\hat{I}_{(p)ij}|^2, \tag{3.115}$$

(3.116)

we get

$$F(\mathrm{e},) = 1 + \frac{62}{3}e_t^2 + O\left(e_t^4\right). \tag{3.117}$$

For the enhancement function χ, the summation of $\ln(p/2)\times$(Bessel functions(e_t)) needs to be evaluated, i.e.

$$\chi(e) = \frac{1}{64}\sum_{p=1}^{+\infty} p^8 \ln\left(\frac{p}{2}\right)|\hat{I}_{(p)ij}|^2. \tag{3.118}$$

Considering the expansion of $|\hat{I}_{(p)ij}|^2$ in terms of e, up to $e_t^2\,\chi$ is evaluated. One gets,

$$\chi(e_t) = \left(-\frac{77}{3}\ln[2] + \frac{6561}{256}\ln[3]\right)e_t^2 + O\left(e_t^4\right), \tag{3.119}$$

in complete agreement with Eq. (3.114e) of the previous section.

Similar calculations for the tail terms yields the following results:

$$\mathcal{F}_{MQ} = \frac{32}{5}\nu^2 x^5\left\{4\pi\left(1 + \frac{2335}{192}e_t^2\right)x^{3/2} + \pi\left(-\frac{428}{21} + \frac{119275}{336}e_t^2\right)x^{5/2}\right\}, \tag{3.120a}$$

$$\mathcal{F}_{MO} = \frac{32}{5}\nu^2 x^5\left\{\pi\left(\frac{16403}{2016} - \frac{25283}{168}e_t^2\right)x^{5/2}\right\}, \tag{3.120b}$$

$$\mathcal{F}_{CQ} = \frac{32}{5}\nu^2 x^5 \left\{\pi\left(\frac{1}{18}+\frac{5}{3}e_t^2\right)x^{5/2}\right\}. \tag{3.120c}$$

Summing up the contributions, we have:

$$\mathcal{F}_{tail} = \mathcal{F}_{MQ} + \mathcal{F}_{MO} + \mathcal{F}_{CQ} \tag{3.121a}$$

$$\mathcal{F}_{tail} = \frac{32}{5}\nu^2 x^5 \left\{4\pi\left(1+\frac{2335}{192}e_t^2\right)x^{3/2} - \frac{8191}{672}\pi\left(1-\frac{138538}{8191}e_t^2\right)x^{5/2}\right\}. \tag{3.121b}$$

From the result above, we obtain:

$$\varphi(e,) = 1 + \frac{2335}{192}e_t^2 + O\left(e_t^4\right), \tag{3.122a}$$

$$\psi(e_t) = 1 - \frac{138538}{8191}e_t^2 + O\left(e_t^4\right). \tag{3.122b}$$

Eqs. (3.114c) and (3.122a) are in agreement, but Eqs. (3.114d) and (3.122b) are in disagreement.

To diagnose this disagreement in the ψ function, let us numerically compare the values of the enhancement function computed in three different ways: Our full original MPM calculation, the numerical comparison in the test particle limit of the previous section and finally the analytical test particle limit calculation in this section. We have:

e,	From the Numerical Calculation	By comparing	Analytically
0.05	0.9925441991498114	0.9929837626663411	0.957716396044439
0.1	0.9645969066891098	0.9719350506653645	0.830865584177756

An examination of this table shows that the first and second column are in adequate agreement but the third column is different. Most probably there is some algebraic error in the analytical coefficients computed here and we hope to recalculate the tail terms analytically and sort out the discrepancy in the ψ function and compare it with Eq. (3.114c), which we feel is correct.

3.11 Conclusion and future directions

The far-zone flux of energy contains hereditary contributions that depend on the entire past history of the source. Using the Multipolar post-Minkowskian wave generation formalism, we have proposed and implemented a semi-analytical method to compute the hereditary contributions from the inspiral phase of a binary system of compact objects moving in quasi-elliptical orbits up to 3PN order. The method explicitly uses the 1PN quasi-Keplerian representation of elliptical orbits and crucially exploits the implicit double periodicity of the

motion to average the fluxes over the binary's orbit up to **3PN** order. Together with the instantaneous contributions evaluated in the previous chapter, it provides crucial inputs for the construction of ready-to-use templates for binaries moving on quasi-elliptic orbits, an interesting class of sources for the ground based gravitational wave detectors and especially space based detectors like LISA.

The extension of these methods to compute the hereditary terms in the **3PN** angular momentum flux and **2PN** linear momentum flux is the next step required toward the above goal. These are presently under study.

The extension of our methods to compute the **3.5PN** terms for elliptical orbits is currently not possible due to the incompleteness of the generation formalism at this order for general orbits. It would also require the use of the **2PN** generalised quasi-Keplerian representation for some of the leading multipoles and thus be more algebraically involved than the present analysis.